INL/EXT-16-40614

Smoothed-particle Hydrodynamics based Wind Representation

Stephen Hess, Linyu Lin, Ram Sampath,
Steven Prescott, Curtis Smith

December 2016

The INL is a U.S. Department of Energy National Laboratory
operated by Battelle Energy Alliance

INL/EXT-16-40614

Smoothed-particle Hydrodynamics based Wind Representation

Stephen Hess, Linyu Lin, Ram Sampath, Steven Prescott, Curtis Smith

December 2016

Idaho National Laboratory
Idaho Falls, Idaho 83415

http://www.inl.gov

Prepared for the
U.S. Department of Energy
Under DOE Idaho Operations Office
Contract DE-AC07-05ID14517

CONTENTS

FIGURES

TABLES

ACRONYMS

AEP	annual exceedance probability
ANS	American Nuclear Society
ASME	American Society of Mechanical Engineers
CCDP	conditional core-damage probability
CDF	core-damage frequency
CFD	computational fluid dynamics
DNS	direct numerical simulation
DOE	(United States) Department of Energy
EDG	emergency diesel generator
EPRI	Electric Power Research Institute
ET	event tree
ELAP	extended loss of offsite alternating-current power
FT	fault tree
GL	generic letter
HRA	human-reliability analysis
HW-PRA	high-winds probabilistic risk assessment
INPO	Institute of Nuclear Power Operations
IPEEE	individual-plant examination of external events
LERF	large early-release frequency
LES	large eddy simulation
LOOP	loss of offsite power
LWRS	Light-water reactor sustainability
NPP	nuclear power plant
NRC	(United States) Nuclear Regulatory Commission
PCIS	primary-containment isolation system
PRA	probabilistic risk assessment
RANS	Reynolds-averaged Navier-Stokes
RG	regulatory guide
RIS	regulatory issue summary
RISMC	risk-informed safety-margin characterization
SDC	shutdown cooling
SPAR	standardized plant analysis risk
SPH	Smoothed-particle Hydrodynamics

SSC	structures, systems, and components
TMSC	Tornado Missile Strike Calculator
U.S.	United States
V&V	verification and validation

1. BACKGROUND

The publication of WASH-1400, "The Reactor Safety Study," (NRC 1975) served as a watershed event in the development and application of probabilistic risk assessment (PRA) at commercial nuclear power plants (NPPs). Subsequent performance of PRA studies and adoption of the technology by both the NPP owner-operators and regulatory authorities has resulted in significant improvements in NPP safety over the past several decades, as measured by the standard metrics of core damage frequency (CDF) and large early-release frequency (LERF). A study conducted in 2008 by the Electric Power Research Institute (EPRI) estimated that from 1992 through 2005 the industry average CDF decreased by approximately 80% from an average of 9.0E-5 to 2.0E-5 per reactor year (J. P. Gaertner 2008). It is notable that this study provided additional evidence for this conclusion by analyzing the annual occurrences of safety-significant events over this timeframe and observed an approximate 80% decrease in such events.

However, until recently NPP PRAs have focused on the response of plant structures, systems, and components (SSCs) to events resulting from internal transient and accident initiators. Assessments of the response of plant SSCs to externally generated events (e.g., earthquakes, floods, high winds and other natural phenomena) have been much less detailed: the assessments were either qualitative in nature or, if quantitative, used conservative bounding-type assumptions. Because the natural phenomena which may generate external challenges to NPP safety and the plant responses to these challenges are not well understood, such analyses possess large uncertainties in the input data and analysis results. As a result, there is much debate over what conclusions can be obtained from such assessments.

The most comprehensive assessments of external hazards to date were performed at U.S. NPPs in response to the Nuclear Regulatory Commission (NRC) Generic Letter (GL) 88-20, Supplement 4 (NRC 1991). This supplement to GL 88-20 required all U.S. NPP licensees to assess and report to NRC "all plant-specific vulnerabilities to severe accidents caused by external events." The external events to be considered in these assessments were seismic events, internal fires, high winds, floods, and other external initiating events, including accidents related to transportation or nearby facilities and any hazards that the licensee identified as being unique to the NPP. The requirements specified in GL 88-20, Supplement 4 are conventionally referred to as the Individual Plant Examination of External Events (IPEEE) Program.

The objective of the IPEEE was to provide the NRC with information from which they could determine whether the licensees' programmatic assessments were capable of identifying severe accident vulnerabilities to externally induced events. The IPEEE also was intended to determine the extent to which cost-effective safety improvements could be implemented to either eliminate or reduce the impact of the identified vulnerabilities. Although the NRC did not attempt to validate the results of a licensee's IPEEE analysis, a comprehensive review was conducted. The results of this assessment and the insights obtained were published in NUREG 1742 (NRC 2002).

1.1 Tohoku Earthquake

On 11 March 2011, the combination of a major seismic event (the Great Tohoku Earthquake) and subsequent tsunami led to core damage events at three units at the Fukushima Dai-ichi NPP in Japan. This accident has been studied in detail by numerous organizations, generating a wide range of recommendations to enhance NPP safety as a result of the lessons learned from the events which transpired as a result of this combination of beyond-design-basis external hazards (Institute of Nuclear Power Operations 2011); (C. Miller 2011); (K. Huffman 2012); (ANS 2012); (ASME 2012); (IAEA 2015). In addition, the earthquake and subsequent tsunami also impacted the four units at the nearby Fukushima Dai-ni NPP. Although significant damage to critical plant SSCs was sustained (nearly all of which was due to flooding from the tsunami), the plant staff was able to take mitigative actions and avoid core damage. This event has been studied less extensively than that at Fukushima Dai-ichi; however, a number of important insights have been gained from this event as well (Huffman 2011).

A critical insight that was obtained (and cited in the reports referenced in the previous paragraph) as a result of the events at the Fukushima NPPs was that much more attention is needed to assess the risks that occur due to externally induced hazards. The results of these assessments have led to a much greater appreciation that such hazards can result in rare but credible events that may lead to core damage and the subsequent release of radioactive materials to the environment. As a result, NPP owner-operators and regulatory authorities around the world have initiated efforts to reassess plant vulnerabilities to external hazards and to identify appropriate actions that should be taken to mitigate their impact on NPP safety.

1.2 Regulatory Impact

As previously indicated, in the United States, the NRC performed a thorough review of the Fukushima Dai-ichi accident and developed a comprehensive set of recommendations for consideration by the Commissioners for implementation as new or revised regulatory requirements (C. Miller 2011). Because of the number and scope of the recommendations, they were prioritized into three tiers for purposes of resource allocation and timing of their resolution. Tier 1 consisted of those recommendations which could "be started without unnecessary delay and for which sufficient resource flexibility, including availability of critical skill sets, exists" (NRC n.d.). Tier 2 actions consisted of those recommendations which were not considered to need long-term technical evaluations but that could not be initiated in the near term due to several factors including the need for additional technical assessment of the issue, the issue's dependence on the resolution of a related Tier 1 issue, or the lack of availability of critical expertise to support addressing the issue. Finally, Tier 3 predominantly consisted of actions that would require further study to support a regulatory conclusion or action. With respect to specific external hazards, an assessment of seismic and flooding events was classified as a Tier 1 action. All other external hazards (including high-wind-related events) were classified as either Tier 2 or Tier 3.

High winds pose a potential hazard for NPP sites around the world. In general, the high-wind hazard occurs in three distinct forms: (1) tornados, (2) tropical storms (i.e., hurricanes and typhoons), and (3) straight-line winds (e.g., from thunderstorms and extratropical cyclones). In many countries, criteria for protection against high wind related hazards were not in place at the time the current fleet of operating NPPs was constructed. Additionally, even in cases where such criteria did exist, there has been a substantial subsequent evolution in them. Operating experience has shown that high-wind events have been responsible for extended losses of offsite AC power (ELAP) events at several NPP sites while simultaneously impacting the plant's ability to cope with these events. The two most significant instances of such events in the United States were the landfall of Hurricane Andrew at the Turkey Point NPP site in 1992 and the significant damage to offsite power circuits at the Browns Ferry NPP due to severe weather and tornados that occurred during the spring of 2011. To illustrate the potential impact of high-wind events at a NPP site, each of these events will be described briefly.

2. HISTORIC HIGH WIND EVENTS ON NUCLEAR POWER FACILITIES

2.1 Hurricane Andrew – Turkey Point

On 24 August 1992, Hurricane Andrew made landfall on the coast of Florida. This event was unique because the eye of the storm passed over the Turkey Point NPP site. The hurricane was a category 4 tropical cyclone with sustained winds of up to 233 km/h (145 mph) with gusts of 282 km/h (175 mph) (NRC 1993). The hurricane resulted in significant onsite damage at the NPP plant site and extensive damage to the area surrounding the facility.

The Turkey Point site is situated on the shore of Biscayne Bay approximately 2 miles east of Homestead, FL. The site is located in the Miami–Dade County region of south Florida, approximately 40 km (25 miles) south of the city of Miami. At the time of the event the site consisted of four electric generating units. Two of the units (Units 1 and 2) are fossil plants whereas the other two (Units 3 and 4)

are three-loop Westinghouse pressurized-water reactor NPPs. (Note that since the event, the facility owner has added a combined-cycle natural-gas-fired plant (Unit 5). At the time of this report, the facility owner is investigating the addition of two additional NPP units to the site.)

As noted previously, the direct impact of the storm resulted in significant on- and offsite damage. The most significant impact to the NPP was the loss of all offsite power for more than 5 days. Additionally, the nuclear portion of the facility was impacted by a complete loss of communication systems, closing of the site-access road, and damage to the plant fire protection system, security systems, and warehouse facilities. The NPP experienced no damage to the safety-related systems except for minor water intrusion (NRC 1993). However significant damage to non-safety-related SSCs occurred. This included (NRC 1994):

- Collapse of the six steel-framed turbine canopies,
- Failure of radioactive-waste building ductwork to the vent stack due to missiles generated as a result of the hurricane-strength winds,
- Collapse of the non-safety-related high-water tank which subsequently fell onto various fire protection system SSCs and rendered one of the fire protection systems inoperable,
- Major structural damage to one of the fossil units' exhaust chimneys. (A photograph of the damaged stack is provided in Figure 1.

Figure 1. Structural damage to Turkey Point Unit 1 exhaust stack. (Union of Concerned Scientists 2011).

2.1.1 Safety Response

As a result of the impact of Hurricane Andrew on the Turkey Point NPP, the U.S. NRC and the commercial nuclear power industry (through the Institute of Nuclear Power Operations [INPO]) formed a joint team to assess the damage caused by the hurricane on the NPP units, review actions taken by the

owner-operator to prepare for the storm and recover from its aftermath, and to identify lessons learned from the event that could benefit other nuclear reactor facilities. Results of this review were provided in the report, "Effect of Hurricane Andrew on the Turkey Point Nuclear Generating Station from August 20–30, 1992," (Hebdon 1993) which was issued in March 1993 and was distributed by INPO to all U.S. power reactor licensees.

There were a number of important lessons learned from the event. These are described in detail in references (NRC 1994); (NRC 1993); (Hebdon 1993). The most significant of these are as follows. First, the NPP owner-operator made extensive preparations for the hurricane before it made landfall. These preparations led to initiation of a plant shutdown approximately 12 hours before the predicted landfall of the hurricane. As a result, both units were in a stable shutdown condition (Mode 4–hot shutdown) when the hurricane impacted the NPP site. Due to the extensive devastation of the local infrastructure in the vicinity of the plant site, the plant owner-operator also took numerous actions to establish necessary infrastructure support to provide the means for plant staff to report to the plant to support cleanup and recovery efforts after the hurricane. In reference (NRC 1993), it was noted that the requirements for such actions "could be more extreme following other external events (e.g., severe earthquake) for which there was no warning to permit advance preparations, including the evacuation of families of plant personnel." The second significant insight obtained as a result of the analysis of this event was that failure of non-safety-grade SSCs could have a significant impact on other plant SSCs that would be relied upon to maintain adequate plant safety. This led the NRC to issue a supplement to the original Information Notice (i.e., reference (NRC 1994)) that emphasized the importance of assessing the potential impact of failures of non-safety-related SSCs under conditions that could occur during events caused by extreme external hazards that could potentially disable plant capabilities to maintain the reactor in a safe showdown condition and any compensatory measures that would be taken by the NPP to mitigate such conditions if they were to occur.

2.2 Severe Weather and Tornadoes—Browns Ferry

Over a period of four days (25–28 April 2011) more than 200 tornadoes occurred over 5 states in the southeastern United States. Of these tornadoes, 15 were classified as EF-4 or EF-5 on the enhanced Fujita intensity scale. The most severe outbreak occurred on the afternoon of 27 April with a total of 122 tornadoes. These tornadoes resulted in 316 deaths, more than 2400 injuries and damage in excess of $4.2 billion (Hayes 2011). A map of these tornado tracks is provided in Figure 2.

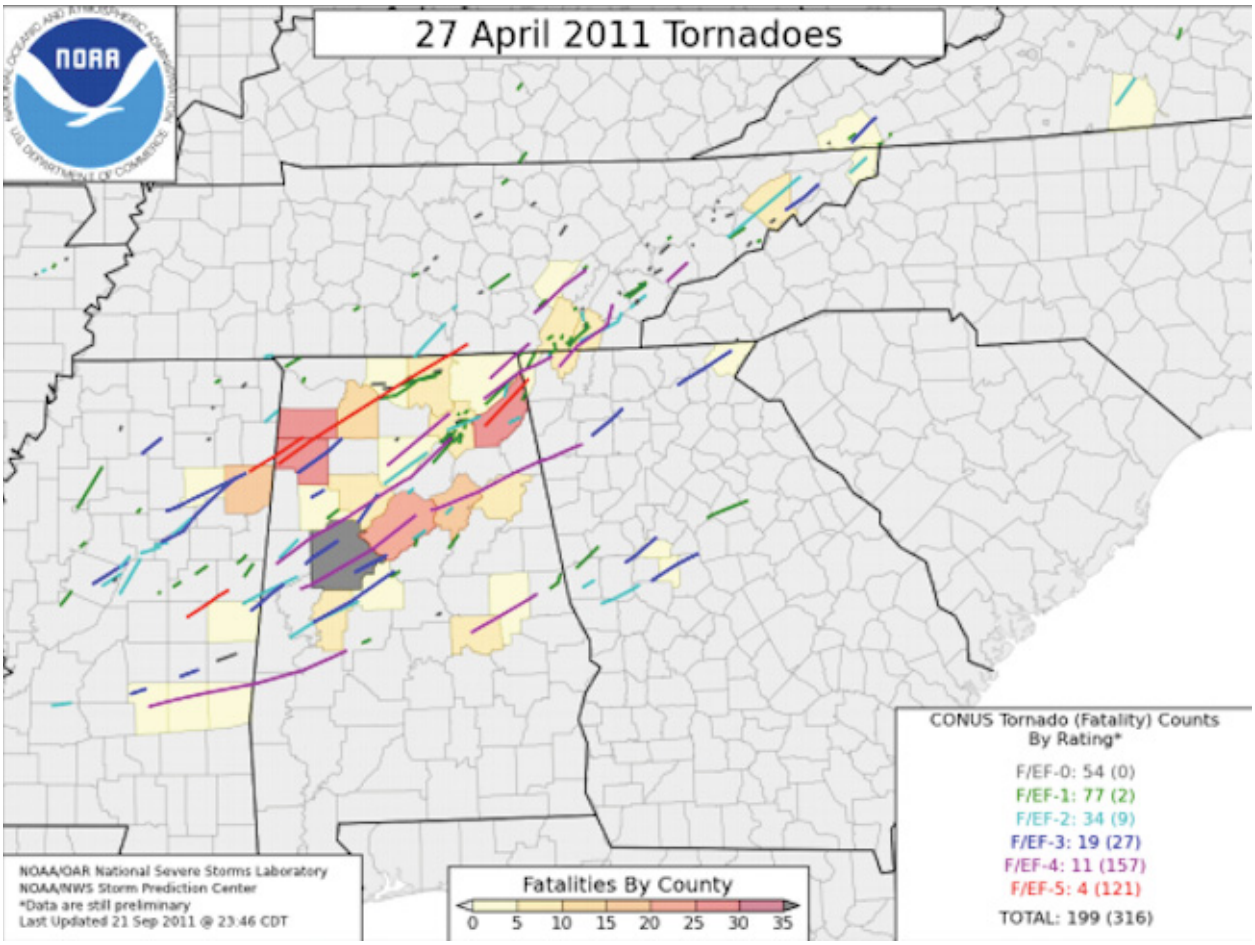

Figure 2. Tornado tracks from 27 April 2011 (U.S. National Oceanic and Atmospheric Administration 2011) (Hayes 2011).

Although the potential for severe weather was forecast by the Storm Prediction Center of the U.S. National Weather Service (with the issuance of tornado watches and warnings in the affected regions), the impact of the tornadoes (particularly the occurrence of a large number of fatalities) was particularly severe due to a combination of reasons. These contributing factors were identified in a service assessment conducted by the U.S. National Weather Service (Hayes 2011). Several of the causal factors that led to the high death toll also were important for the impact on the electrical transmission system and the Browns Ferry NPP. These physical causal factors included the following:

- The occurrence of a large number of relatively rare, long-track, and violent tornadoes
- The rapid speed of propagation of the storms (45–70 mph [72–113 km/hr])
- The occurrence of tornado tracks that intersected with areas of high population density.

In many cases, the high rate of fatalities and injuries could be attributed to human and sociological factors with respect to the response by members of the public to the tornado watches and warnings that were issued in advance of the storm. A detailed assessment of these factors is presented in the U.S. National Weather Service report (Hayes 2011).

The Browns Ferry NPP is located on the Tennessee River in northeastern Alabama, near the town of Athens and approximately 32 miles west of the city of Huntsville, AL. This location is in the middle of the region impacted by storms that occurred throughout the southeastern U.S. during this period of time.

The site contains three General Electric boiling water reactors with Mark I containments. On 27 April 2011, the greater Tennessee Valley region (which includes the Browns Ferry NPP site) experienced severe weather from this system. The tornadoes destroyed a significant number of the Tennessee Valley Authority's transmission poles, towers, and lines, including most of those that serve as the primary source of offsite power for Browns Ferry. Offsite power was lost to Units 1 and 2 of the NPP and, although a single 161 kV line remained available to provide offsite power to Unit 3, the station treated the event as a complete loss of offsite power to that unit as well (Wierman 2013). The event resulted in a loss of all 500 kV offsite power at the plant site and a reactor trip on each of the three units. AC power to critical NPP systems was supplied, as designed, by onsite emergency diesel generators (EDGs), and the reactors were cooled and depressurized, reaching a cold-shutdown condition the following day (28 April). The only safety-significant issue encountered between the time that cold shutdown was achieved and offsite power was restored was the need for plant personnel to execute a rapid shutdown of the Unit 1 and 2 C EDG due to a hydraulic oil leak in piping for the EDG governor that caused fluctuations in the generator output voltage. This action resulted in a loss of shutdown cooling (SDC) to Units 1 and 2 due to a primary-containment isolation system (PCIS) signal that occurred during the shutdown of the EDG. SDC was restored to Unit 2 within a very short time and to Unit 1 within 47 minutes of the event. The C EDG was repaired and returned to service on 29 April. Offsite power was restored, and the EDGs were secured, on 2 May (NRC 2016).

3. ASSESSMENT OF HIGH WINDS IMPACTS ON NUCLEAR PLANT SAFETY

3.1 Current Approach to Performing High Winds PRA

The standard approach to assess the risks of external hazards (including high winds) to NPPs is to conduct a hazard-specific PRA and integrate the results into the NPP's existing PRA model. In this framework, the conduct of a PRA for an external hazard comprises three elements:

1. Conduct of a hazard analysis to determine the frequency or annual exceedance probability (AEP) of different levels of the hazard under study. For application to high winds, this consists of analysis of the high wind characteristics for the NPP site and estimating the AEP for winds at various speeds. The results of this analysis are the generation of one or more high-winds hazard curves that are applicable to the NPP.
2. Evaluation of the strength and response of plant SSCs to the particular hazard. In a high-winds PRA (HW-PRA) this consists of evaluation of wind loads and the effects of impacts of wind-driven missiles on vulnerable SSCs to determine their failure probabilities due to these phenomena. The results of this analysis are fragility curves for the various SSCs that are susceptible to the effects of the winds or wind-generated missiles.
3. Development of a hazard-specific fault-tree or event-tree (FT/ET) model to evaluate the risk associated with the particular hazard. In the context of an HW-PRA this includes the incorporation of results from the first two steps described above and integration of these hazard-specific models into the NPP's PRA.

In the current state of practice, the detailed assessment of a specific external hazard at a particular NPP site would only be performed if the hazard is expected to provide a non-negligible contribution to the risk metrics obtained from a PRA model. In practice, this implies that the hazard does not meet the requirements specified to screen out hazards that are considered to be negligible. A number of approaches for the conduct of such screening have been developed and applied at operating NPPs. In the U.S., most NPP owner-operators have applied the approach developed in 2011 by EPRI (L. Shanley 2011) (with subsequent update to reflect utility experience and lessons learned that was published in 2015 (EPRI 2015)). Experience obtained from NPP applications of this screening process indicates that because of the ubiquitous nature of high-wind events and the potential impact that extreme wind events can have on

exposed NPP SSCs, the high-wind hazard would not screen out and, thus, requires a more extensive analysis.

In their structure and application, HW-PRAs are often compared with seismic PRAs. The ASME/ANS standard on probabilistic risk assessment for NPP applications (ASME/ANS 2013) notes that the requirements for a HW-PRA are similar to the requirements for seismic PRAs, with some adaptations that reflect the differences between the characteristics associated with the two hazards. For NPPs, high winds are significant because they may result in an initiating event that may present a challenge to plant safety. One typical NPP event that may occur as a direct result of the high-wind hazard is a loss of offsite power (LOOP) due to the impact of the high winds on the electrical-transmission system. Note that an extended LOOP was one of the outcomes of the high-wind events at Turkey Point and Browns Ferry discussed previously. The likelihood of events that may impact NPP safety is determined in the plant hazard analysis. In addition to initiating a plant transient, high winds also may result in direct or indirect (i.e., via wind-borne missiles) damage to one or more SSCs that are important to plant safety. Within the plant PRA model, the likelihood for the creation of wind-driven missiles and their impact on SSCs is evaluated in the missile-hazard analysis. The impact of the high winds and subsequent wind-driven missiles on the plant SSCs (i.e., resulting in damage to or failure of them) is determined using fragility-analysis techniques, similar to those that are used in seismic-risk assessments. In a high-winds fragility analysis, the variable of importance is the wind speed (whereas, in a seismic-risk assessment, SSC fragilities are dependent upon the magnitude, frequency, and temporal duration of ground motion). The convolution of the wind hazard with the SSC fragility is accounted for in the plant response model, which typically is developed from the site internal-events PRA. In addition to the wind- and missile-related SSC failures, random equipment failures and the failure of operator and other recovery actions are accounted for in the HW-PRA. Quantification of the risk (i.e., via estimation of applicable metrics such as CDF and LERF) is performed in a manner similar to that used in the conduct of the plant internal-events PRA. This process is displayed schematically in Figure 3, which is taken from (NRC 1983).

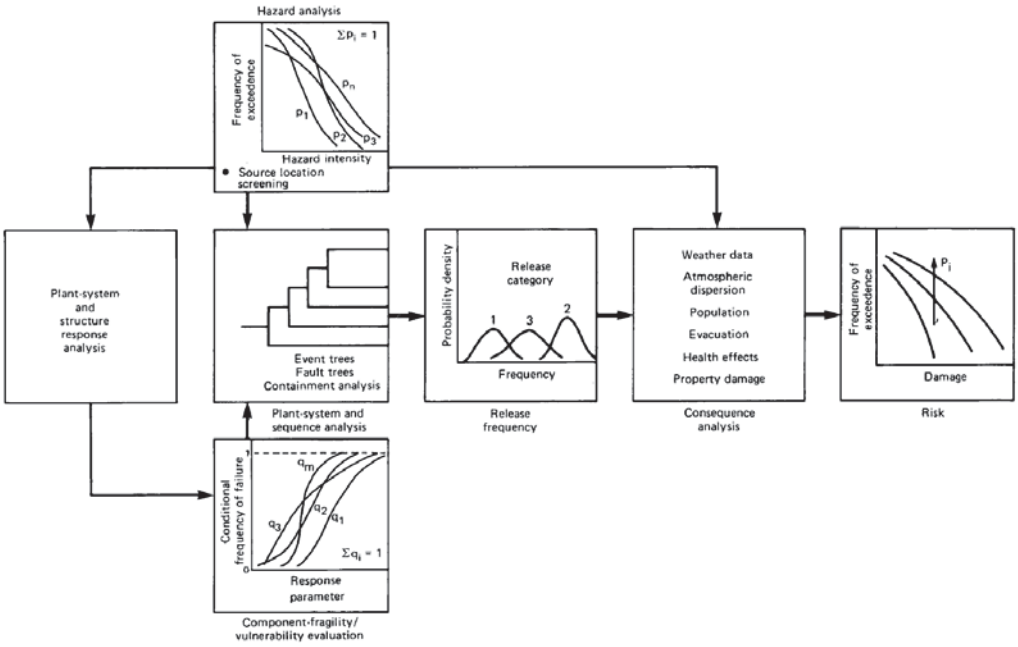

Figure 3. Overview of external-hazard PRA from Figure 10-1 of NUREG/CR-2300 (NRC 1983).

Of the three steps required to perform a HW-PRA, the most challenging is that related to assessing the likelihood and impact of the hazard (both the direct effect of the wind hazard and the effect of a

missile impact) on a particular SSC. This portion of the analysis has proven to be technically challenging, labor intensive, and costly to perform. Initial work in this area was conducted in the late 1970s and early 1980s under the sponsorship of EPRI. This effort led to the development of the TORMIS (EPRI 1978) and TORRISK (L. A. Twisdale 1983) computer codes.

Because of the robust design associated with commercial NPPs, a significant portion of the impact of high-wind events on these facilities is due to wind-generated missiles. Because the most significant (i.e., highest-kinetic-energy) missiles of this type are generated from tornadic events, protection against this hazard is specified in the NPP design basis. For missiles generated by tornadoes, the U.S. Nuclear Regulatory Commission provides information on acceptable design and acceptance criteria in Regulatory Guide (RG) 1.76 (NRC 2001). This guidance document defines a range of projectiles (i.e., it specifies a spectrum of design-basis missiles) and corresponding impact velocities that have been determined to be acceptable by the U.S. regulatory authority to assess the effects of missiles that may be generated by the occurrence of a tornado at or near an NPP site. Similar guidance recently has been developed for design-basis protection against hurricanes and hurricane-generated missiles; this guidance is being applied to the licensing of new NPPs under construction in the United States (NRC 2011).

In the assessment of the impact of wind-driven missiles to NPP SSCs, the probability of missile damage is dependent upon several variables. These factors include the intensity (speed and duration) of the wind, the exposed surface area of the target SSC, and the number and type of missiles that may be generated (called the missile inventory). The physics of the event has the following discrete components:

1. Injection of a missile into the wind stream
2. Transport of the missile through the air to the exposed SSC
3. Response of the SSC to the missile impact.

The missile impact hazard represents steps (1) and (2) in this sequence and results in the conditional probability of a wind-generated missile impacting a specific, vulnerable SSC given the occurrence of a tornado strike on or near an NPP site. Step (3) represents the fragility of the SSC to the given missile strike. In the application to NPP PRAs, a range of approaches have been used to assess the effects of wind-driven missile impacts. TORRISK/TORMIS constitutes a modeling and simulation approach that uses random variables to physically model the inherent variations in tornado incidence, wind field characteristics, missile position, missile orientation, missile transport, and the distribution of the potential missile population. The methodology uses missile time-history simulations to predict the response of the missiles to the tornado as it moves in the vicinity of the NPP site. Because the TORRISK/TORMIS approach is statistical, the performance of sensitivity studies is an essential component of its application. In the original demonstration analyses, numerous sensitivity cases were run. These included varying (among other variables) the missile-population size and missile types, the Monte Carlo sample sizes, and the variables associated with missile transport phenomena (EPRI 1978). The result of a TORRISK/TORMIS analysis is an estimate of the probability of a tornado-generated missile striking each modeled NPP SSC (with various confidence-interval estimates) over different wind speed ranges given the plant geometry and the input missile population at the site. In the performance of a TORRISK/TORMIS assessment, the missile input population and missiles spatial distribution across the site is obtained from a detailed site walkdown. In the assessment of the risks due to wind-driven missiles at commercial NPPs, most analyses have employed the TORRISK/TORMIS computer codes. However, as a result of regulatory experience with submittals from some licensees, the U.S. Nuclear Regulatory Commission has provided generic information that describes issues that have occurred in the use of these codes and the interpretation of results and to clarify NRC expectations for licensees that conduct such analysis for the purposes of regulatory submittals (NRC 2008).

Because of the complexity and expense associated with the conduct of a HW-PRA, simplified approaches to address the issue of assessing the likelihood of wind-generated-missile strikes on plant

SSCs have been investigated. This is particularly important as, to date, there are only two methods that have been determined to be acceptable to the U.S. NRC to ensure SSCs required for safe shutdown and reactor cooling have adequate protection against wind-generated missiles: (1) implementation of physical protection or (2) a risk analysis which demonstrates that the risk associated with the vulnerability is sufficiently low (NRC 2015). For SSCs identified to require such design-basis protection, the first approach would require incurring significant costs of installing plant modifications while, to date, the second approach has required use of TORRISK/TORMIS (and which also has been found to be expensive with a significant level of regulatory uncertainty associated with the level of analysis detail required to obtain regulatory approval). The basis for such alternative approaches is that, although the risks to commercial NPPs from high-wind events and wind-generated missiles is not negligible, these risks are expected to be significantly smaller than that due to seismic and flooding events. Such expectations were confirmed in a recent simplified risk assessment conducted by the U.S. NRC (NRC 2014) as part of its efforts to ensure adequate design-basis protection against tornado-generated missiles, as described in Regulatory Information Summary (RIS) 2015-06 (NRC 2015).

One recent effort was the development of a simplified computer spreadsheet application to support HW-PRAs conducted by Westinghouse Electric Corporation. This effort resulted in the development of the Tornado Missile Strike Calculator (TMSC). This Microsoft Excel-based application is intended to be user-friendly and to permit development of missile-strike probability estimates that can be input into NPP PRAs with less effort and computational requirements than the TORRISK/TORMIS Monte Carlo simulation approach. Example results from application of this tool to a hypothetical NPP have been presented in a recent conference paper (K. Hope 2015). At this time, work on the application—particularly on benchmark and validation activities—continues; however, unlike the application of the TORRISK/TORMIS approach, the use of TMSC has not been reviewed or accepted for licensing submittals by the U.S. NRC. Although this approach has promise to significantly reduce HW-PRA analysis costs in the short run, because it relies on statistical correlations (i.e., the application does not explicitly model the fundamental physics of the phenomena), it likely will only be applicable to address issues that are within its documented validation basis.

3.2 Results and Insights from Recent High Winds Risk Assessments

The accident at the Fukushima Dai-ichi NPP in 2011 has resulted in an enhanced focus on the potential impact of external hazards on NPP safety. Although seismic and flooding events (which were the direct causes of the Fukushima accident) have been the primary focus of both regulatory authorities and NPP owner-operators, several HW-PRA risk assessments have been performed in the past several years. In this section we present a brief summary of the results and insights obtained from these studies.

As indicated previously, in 2014 the U.S. Nuclear Regulatory Commission performed a limited simplified risk assessment of the risks associated with tornado generated missiles (NRC 2014). This study was conducted to inform regulatory decision-making on the specification of timeframes under which licensees would need to take actions to ensure their NPPs were in compliance with their approved licensing basis. This study made a number of bounding assumptions and simplifications to assess whether non-conformances that had been identified by some NPP owner-operators constituted an immediate safety concern for which the NRC would need to take prompt action. In the NRC study, tornado-strike hazard curves from NUREG/CR-4461 (NRC 2007) were used to provide a bounding estimate of the initiating event frequency for generation of a damaging tornado missile in each of the three tornado regions specified in that report. The analysis then applied the NRC's standardized plant-analysis risk (SPAR) models for several representative NPPs to analyze failures of SSCs that had been found not to meet the licensing basis for tornado-missile protection at several operating NPPs. The following steps were performed to conduct the simplified bounding risk assessment (NRC 2014).

- Select a sample of NPPs located in the region with the highest tornado hazard

- Apply the internal events loss of offsite power (LOOP) event tree from the sample NPPs SPAR model to perform the risk analysis
- Remove any credit for offsite power recovery and solve the event tree to determine the base case conditional core damage probability (CCDP) given the occurrence of the LOOP event with no recovery of offsite power
- Fail the identified selected SSCs that are assumed to be unprotected from tornado missiles and calculate the new CCDP
- Estimate the change in CDF that is attributable to the assumed SSCs not being protected from tornado missiles by multiplying the increase in CCDP over the base case by the bounding initiating event frequency.

To obtain results that would be considered bounding, the following conservative assumption were made:

- The upper bound on core-damage risk for the tornado-missile hazard was set at the frequency at which a tornado with wind speeds in excess of 75 mph (121 km/hr) would strike the representative NPP site
- Unprotected safety-related SSCs are assumed to fail with certainty (i.e., a SSC fragility set equal to 1) for any missiles that hit the SSC that are generated from tornadoes with wind speeds greater than 75 mph
- Any non-safety-related SSCs that might fail from a tornado missile are assumed to fail in all cases analyzed.

In addition to the analyses described above, several sensitivity studies were conducted to provide additional confidence in the results obtained and to support application of the results in the regulatory decision-making process.

In the NRC's bounding risk assessment, seven NPPs located in NRCs Tornado Region III (as described in (NRC 2007)) were selected. All of these NPPs are located in the region of the U.S. with the highest rates of tornado occurrence (i.e., the central U.S. region). The seven plants include both boiling-water reactor and pressurized-water reactor types with representative NPPs from each of the major nuclear reactor vendors. The representative vulnerable SSCs were selected from SSCs that had previously been identified by the plant licensee and reported to the NRC as not possessing tornado-missile protection as specified in the NPPs licensing basis. Typical examples of these SSCs include intake and exhaust stacks associated with the NPP's EDGs and piping associated with critical plant cooling-water systems (e.g., essential service water, plant closed cooling water, auxiliary feedwater systems). For each representative NPP, at least two cases were assessed: loss of the EDGs and loss of the essential service water functions. Thus, the SSCs assessed in this analysis all possessed high risk importance (and, thus, represented an additional conservatism in the analysis assumptions). The analyses conducted led to the following conclusions:

- Any NPP non-conformance with tornado missile protection licensing basis requirements would not require immediate plant shutdown because the risk is bounded by the initiating event frequency for NPPs located in the most severe tornado region in the US.
- The extremely conservative nature of the analysis indicates that licensees should be given a reasonable time to identify design basis non-conformances and either correct them (via physical protection) or demonstrate via a more complete risk analysis that the risk due to the nonconformance is sufficiently low that physical protection is not required. (In reference (NRC 2015), these timeframes were set at 3 years for NPPs in NRC Tornado region III and at 5 years for NPPs in NRC Tornado Regions I and II.)

It should be emphasized that this analysis and its subsequent application to regulatory decision-making were very limited in scope. Thus, this generic risk assessment does not necessarily reflect the full potential impact of high-wind events on NPP safety.

In addition to this limited bounding risk assessment performed by the U.S. NRC, full scope HW-PRAs recently have been performed at several NPPs with results and insights reported in the literature. These recent papers cover all aspects of performing a full scope HW-PRA, including conduct of NPP-site high-wind walkdowns (J.C. Sciaudone 2015), SSC-fragility modeling and analysis (P. V. L.A. Twisdale 2015), integration into the plant PRA model and assessment of risk results (N. L. L.A. Twisdale 2015), and the insights gained and lessons learned from conduct of a HW-PRA (Lovelace 2015). Information from each of these papers is summarized below.

In the paper from Sciaudone et al. (J.C. Sciaudone 2015), experience obtained from the conduct of high-winds walkdowns at NPPs is discussed. Similar to experience with seismic and flooding hazards, the performance of a comprehensive site walkdown is necessary to identify potential vulnerabilities to the hazard that exist at the NPP site. In addition to identification of potential vulnerabilities to high-wind events, the outcome of the site walkdown includes an assessment of the condition of plant SSCs and identification of potential structural interactions among SSCs. Finally, the high-winds walkdown also generates an inventory of potential missiles. One of the insights obtained from the conduct of site walkdowns has been that a significant portion of the potential missile inventory consists of materials that are located within non-Category 1 structures, but that can be liberated and entrained in the windfield after the structure deconstructs during a high-wind event.

The paper from Twisdale et al. (P. V. L.A. Twisdale 2015) provides an overview of the advances in wind modeling since the occurrence of Hurricane Andrew in 1992. The authors present a discussion of modeling of the wind hazard and note that the current state of the art is to develop separate hazard curves for each different wind source (thunderstorms, extratropical cyclones, tropical cyclones, and tornadoes). Several example hazard curves are provided in the paper. One aspect of the high-wind hazard that is readily apparent is that the hazard curves are all very steep and that as one goes to smaller hazard AEPs (which is equivalent to longer phenomena return periods), the uncertainties can become extremely large. A second important item discussed in this paper is the effect of the correlation of high-wind events with locally intense precipitation, in particular, the effects of rain ingress on SSCs located inside buildings and structures that sustain damage as a result of a high-wind event. Electrical equipment (motor control centers, switchgears, etc.) are particularly vulnerable to the effects of this correlated combination of hazards. Finally, the paper presents a discussion on the assessment and modeling of SSC fragilities. This includes discussion of the fragilities due to wind-pressure effects, wind-driven-missile impacts, progressive failure mechanisms for structural cladding (e.g., roofs and walls), and water ingress.

Next, the paper by Twisdale, Lovelace, and Slep (N. L. L.A. Twisdale 2015) discusses experience in integrating analysis of high-wind hazards into existing NPP PRAs and interpretation of the results for use in risk management and risk-informed decision making. One of the important insights noted in this paper is that the degree of conservatism in the estimated CDF values was dependent upon the level of discretization used in binning the hazard curves for input into and quantification of the NPP PRA model. Because an NPP PRA model uses a discrete ET/FT approach, individual events must be input in this format. The steep slope of the hazard curves associated with high-wind events can result in a significant overestimation of the impact of these events if too gross a discretization is used. For example, for tornadic wind events the enhanced Fujita classification utilizes six discrete windspeed ranges (EF0–EF5). The authors found that, for purposes of performing a NPP HW-PRA, at least 10 discrete windspeed intervals should be used in assessing the wind hazards (and resultant SSC fragilities for each windspeed range) and, in the paper summary, they recommend the use of 15 intervals. Because of the much higher likelihood of occurrence of high-wind events at lower windspeeds and the lower likelihood that a particular SSC would fail during a lower windspeed event (smaller SSC fragilities at lower windspeeds)

the authors recommend biasing the discretization to provide smaller ranges in the lower-windspeed portion of the hazard curves.

Finally, the paper from Mironenko and Lovelace (Lovelace 2015) provides a practical how-to guide for performing an HW-PRA. In this paper, the authors describe the specific activities required to conduct an HW-PRA: (1) development of a high-winds equipment list, (2) conduct of the site high-winds walkdown (including generating a plant-specific missile inventory), (3) performance of high-winds SSC fragility analysis, (4) assessment of the impact of high-winds events in NPP human-reliability analyses (HRAs), and (5) integration into the existing NPP PRA. The paper also provides a bulletized list of lessons learned that is intended to allow for a more efficient and effective conduct of the activities necessary to perform an HW-PRA. Based on the conduct of HW-PRAs that were referenced in this paper, there were several insights that may be generically applicable to any HW-PRA, the most important of these being cited below.

- The safety impact of high-winds events (as measured by CDF) can be dominated by lower-windspeed events that result in an extended LOOP due to the combination of the much higher frequency of occurrence of low-windspeed events combined with the relatively high likelihood of failure associated with the offsite transmission and distribution system (i.e., the electrical grid).
- Based on interviews with plant operations personnel, even for lower-windspeed events, the operators may elect not to perform prescribed plant mitigation actions while the site is experiencing the high wind conditions. This decision may be made regardless of the condition of the plant if the action requires personnel to transit outside of the main control room, thus subjecting the responding personnel to direct physical danger.

4. ADVANCED MODELING OF HIGH WINDS

As described in the previous sections, the assessment of the impact of high-wind events on NPP safety is a complicated and challenging endeavor. The phenomenology is characterized by complex physics, consisting of at least three distinct wind sources (straight-line, tropical cyclone, and tornadic) which possess different physics, have different potential interactions with and effects on NPP SSCs, and possess different correlations to other related hazards. Thus, high winds represent a set of phenomena that has the characteristics of being multi-physics and multi-scale. This is particularly true when the direct effects of the windfield are combined with other correlated hazards, such as locally intense precipitation and wind-generated missiles. The phenomena are also highly complex in both the spatial and temporal realms. For example, in a tornadic event, the intensity of the windfield varies with both the temporal duration of the storm and also within the physical dimensions of the tornado itself. In (L. A. Twisdale 1983), Twisdale and Dunn cite data that indicate, based on an assessment of the resultant debris field, an F5 tornado will only experience F5 force winds over roughly 15% of its track. It is clear from the preceding discussion that such resolution is not achievable using the suite of methods and tools currently used for the performance of HW-PRAs.

4.1 RISMC

As part of the U.S. Department of Energy (DOE) Light Water Reactor Sustainability (LWRS) Program, the Risk-Informed Safety Margins Characterization (RISMC) Pathway is conducting research and development for advanced methods and tools to support NPP safety assessments and management. One area of current research is in applications to address external hazards that can impact NPP safety. This research currently is being performed as an industry application of the RISMC approach (referred to as Industry Application 2). Because the RISMC approach explicitly couples probabilistic approaches (the "scenario") with a phenomenological representation (the "physics") through a modeling and simulation-based approach, it is ideally suited to serve as a framework to address the interactions of external hazards on NPPs and their resultant potential impact on plant safety. Additionally, because the RISMC approach identifies and integrates distributions associated with all of the critical physics that influence the scenario,

characterization of uncertainties is a fundamental and direct outcome of the approach. Thus, the use of the RISMC approach is ideally suited to support the assessment of and decision making associated with external hazards.

For application to high-wind hazards, a large number of physical phenomena are relevant to assessing the hazard and determining its impact at a particular NPP. However, these physics can be categorized into the following:

1. Aerodynamics of the local windfield experienced at the NPP site
2. Structural loading and response of plant structures to the effects of the experienced wind forces
3. Dynamics of wind-generated missiles (lift, flight trajectory, etc.) and whether or not they impact particular plant SSCs
4. Damage imparted to plant SSCs due to impact with a wind-borne missile.

Items (1) and (3) correspond to the issue of hazard characterization discussed earlier in this report while items (2) and (4) address the issue of SSC fragility.

In initial work on the external-hazards industry application, attention was focused on two specific hazards: seismic and flooding. For the flooding portion of this work, investigations were conducted in the potential to apply the smoothed-particle hydrodynamics (SPH) approach to model external flooding events. In 2015, initial research was conducted to evaluate the capabilities of different SPH computer codes and assess their potential utility for use to model flooding phenomenology important to NPP risk and safety evaluations. The result of these investigations indicated that the SPH approach was viable and that several of the codes likely could be adapted to support the assessment of NPP flooding events (C.L. Smith 2015).

The external flooding phenomenon has several commonalities with high winds. First, both phenomena possess complex fluid dynamics. They also are capable of generating fluid-structure interactions that can adversely affect NPP SSCs. Finally, both phenomena have the potential for entraining and transporting debris, which also can impact and adversely affect NPP SCCs. Due to these similarities and because of the encouraging results obtained in the initial assessment of SPH for application to external flooding, the approach was identified as one which could be adaptable for use in assessing the impact of high-wind-related external events at NPPs.

4.2 Smoothed-particle Hydrodynamics

4.2.1 Overview

SPH was originally designed for solving astrophysical problems by Gingold and Monaghan (R. G. Monaghan 1977), and Lucy (Lucy 1977). SPH is a mesh-free Lagrangian fluid-simulation technique. Being mesh-free, SPH does not require a stationary grid when solving the fluid equations of motion. This is in contrast to Eulerian techniques, which require an underlying grid. SPH works by obtaining approximate numerical solutions of the equations of fluid dynamics by representing the fluid with particles, where the physical properties and equations of motion of these particles are based on the continuum equations of fluid dynamics. Further, physical quantities are estimated by interpolating existing fluid quantities using the neighboring particles.

A kernel (or weighting) function with influence radius (or smoothing length) acts as the weighting factor for the contributions from the neighborhood interpolation points.

The SPH approximation is illustrated in Figure 4. The SPH kernel is usually used for computing particle density, where contributions from neighboring particles decrease with increasing distance. For a detailed explanation refer to the comprehensive annual review of Monaghan (J. Monaghan 2005).

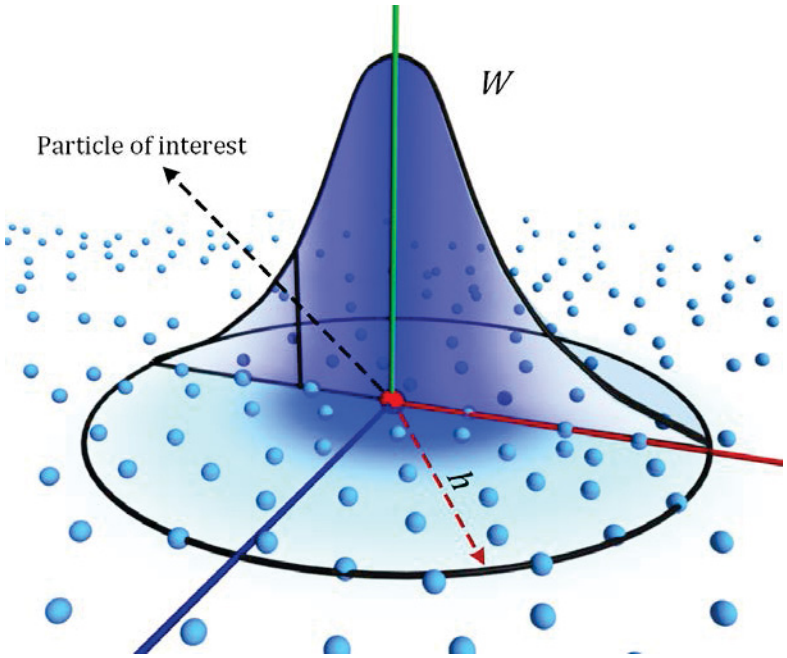

Figure 4. Illustration of SPH approximation for a field variable of the red particle, where *W* denotes a Gaussian-like interpolation function (SPH kernel), *h* is the influence radius (smoothing length).

4.2.2 Fluid Simulations

The use of SPH for fluid simulations has some advantages over other grid-based methods: notably the ability for complex interfaces, such as including fluid-solid interactions and free-fluid surface. The success of SPH in dealing with flow problems is due to its extraordinary ability to simulate a large variety of complex flows, involving a wide spectrum of problems. The main interesting features it possesses are the ability to deal with:

- Distorted and rapidly moving free surfaces without any restriction with respect to their topologies
- Highly nonlinear, inertia-dominated flows and impact processes
- Multi-fluid flows and multi-physics
- Fluid/structure interactions, including rigid-body motion in a fluid and fluid/elasticity coupling.

SPH also lives with the basic principles of Lagrangian and Hamiltonian mechanics**.** SPH has been compared to the traditional numerical methods in computational fluid dynamics (CFD)—typically, finite-difference/finite-element/finite-volume methods combined with volume-of-fluid/level-set methods—which rely on an Eulerian, mesh-based approach. The following are the types of flows in which SPH seems to be preferred. Some of these scenarios occur in dealing with flows involving wind.

- Violent, convection-dominated dynamics
- Large deformation of the fluid domain
- Interactions with geometrically complex structures
- Interactions with highly deforming/moving structures
- Multi-phase processes (e.g., air-water mixtures, sediment flows, granular flows).

Neutrino-SPH

Neutrino-SPH belongs to the class of incompressible SPH solvers which are generally used for subsonic flow involving fluids. Some of the features which Neutrino-SPH has are listed below.

- Ability to handle implicit-incompressible and compressible flows
- Ability to couple other simulations from other 2D/3D domains
  - Coupling with shallow-water code
  - Coupling from varying scales
  - Coupling with Bernoulli's model or Torricelli's model
  - Coupling with rigid body solvers
- Open boundaries for inflow and outflow conditions
- Coupling with other PRA computational systems
- Previous use in industry-level applications involving
  - Pipe breaks
  - Rain-induced flooding
  - Lake breaches impacting structures
  - Lake overtopping
  - Tsunami-induced flooding
  - Room-level flooding affecting components and real-time feedback
- Geometry imports from various architectural/engineering formats.

In spite of its advantages, SPH also has several disadvantages, some of which are listed below

- Large computational times in large 3D domains
- Difficulty in prescribing wall boundary conditions
- Lack of a consistent theory in relation to the mathematical foundation of the method (convergence, stability)
- Difficulties in dealing with variable space resolution for incompressible flows.

4.2.3 Current SPH PRA Research

As part of the RISMC pathway, research was conducted into the use of SPH fluid simulations for flooding scenarios. Demonstrations were performed for large-wave scenarios, dike failure, and internal flooding from pipe failure. In the Industry Application II demonstration, the failures of SSCs within the simulations contributed to PRA results. Refer to (Justin Coleman 2016). Table 1 provides a comparison of the flooding and high-winds hazards and notes any implications for use of SPH to address high winds.

Table 1. Characteristics of high winds and flooding hazards with respect to use of SPH modeling.

Physical Characteristic	Wind	Flooding	SPH Implications
Fluid Density	Low density (air)	High density (water)	Effect of gravity is less and special particle shifting implementation to fill particle voids
Fluid Velocity	Medium to High—Damage to NPP SSCs only at high velocity due to relative low density of air	Low to Medium—Damage to NPP SSCs even at low speeds due to high density of water or due to inundation	Time-stepping restrictions needed for handling high velocity particles
Flow Type	Highly turbulent at damaging wind speeds, including rotational energy for tornadic winds	Low to moderately turbulent	Turbulence handling either k-ε method or sub-particle scale turbulence method implementation.
Spatial Interactions	Limited to SSCs located outside robust structures—SSCs located within industrial grade structures vulnerable after structural elements deconstruct at higher windspeeds	Limited to SSCs located on elevations below the level of flooding	Boundary handling with static structures
Effect of Debris	Significant potential to damage exposed NPP SSCs due to large potential number of potential projectiles and high kinetic energy imparted to them by windfield—in many cases effects of wind-driven missiles are much more likely to damage critical NPP SSCs than the direct effect of the windfield	Typically, a minor contributor compared to direct effects of dynamic pressure (high relative density of fluid) and inundation (particularly for electrical SSCs)	Dynamic rigid fluid-coupling implementation.

4.3 SPH High-winds Investigation

SPH, because it is a particle-based CFD method, is good at simulating complex interfaces, including fluid-solid interactions, free-fluid surfaces, and so on. It has been widely applied in large-scale fluid simulations, and it is proposed as a viable option for high-wind analysis. The objective of this project is to assess and demonstrate SPH-based modeling and simulation capability for analysis of high-wind scenarios less than EF2 scale (<135 mph) windspeeds, which is claimed to be safe in NPP operating basis. This project will also investigate the need for advanced SPH capabilities, including turbulence, solid modeling, and so on.

This research will demonstrate how SPH methods could be used to enhance high-wind simulations for severe accidents, to be used in the RISMC framework. In particular, it is envisioned that SPH can be applied as a simulation tool capable of accurately capturing key features of the high-wind hazard to NPPs including: 1) wind flow pattern and 2) interaction between wind and the solid objects. Such capability to evaluate the interactions of the high-wind phenomena with NPP SSCs is needed before the probabilistic analysis can be performed.

4.3.1 Phenomenon Decomposition and Ranking

In order to accurately represent the high-wind phenomenon, the phenomenon is decomposed into smaller components, as shown in Figure 5. And to better represent each component, specific models or solution methods are required for application of the SPH approach. Except for the laminar flow model, which has been developed and verified in SPH for a long time, new models, such as SPH turbulence and solid models, are needed.

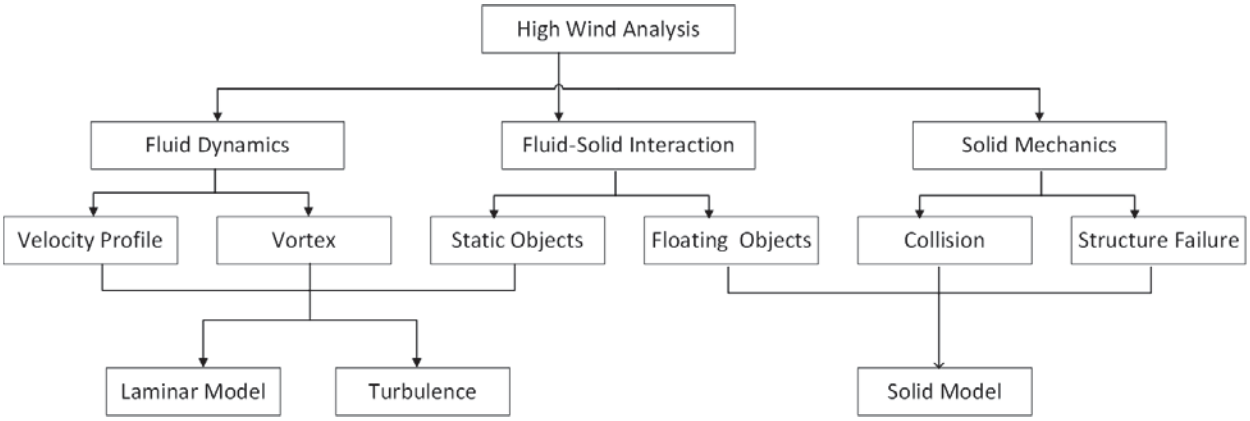

Figure 5. Phenomenon decomposition and possible models needed for application of SPH to high-winds phenomena.

After the phenomenon decomposition, the phenomena identification and ranking table (PIRT) process is applied to identify and prioritize important physical phenomena in an application and to assess the adequacy of and gaps in the current simulation capabilities. This process helps to ensure both sufficiency and efficiency by expert elicitation and prioritization of the analysis of the simulation and experimental capabilities (Laboratories n.d.). The process also has been accepted as an integral part of the conduct of safety analyses at NPPs (and regulatory review thereof: see for example (NRC 2005)). A summary initial high-level PIRT for application of SPH to high-wind phenomena is provided in Table 2.

Table 2. High level PIRT for application of SPH to high wind phenomena.

Phenomenon	**Decomposition**	**Importance**	**Adequacy**	**Validation**
Fluid Dynamics	Velocity Profile	High	Medium	Low
	Vortex	High	Low	Low
Fluid-Solid Interaction	Flowing Objects	High	Medium	Medium
	Static Objects	High	Medium	Medium
Solid Mechanism	Collision	Medium	Medium	Medium
	Structure Failure	Low	Low	Low

As a result, more work is needed for fluid dynamics, especially the vortex problem. Some work has been done on development of turbulence models in SPH (Ferrand 2011, Leroy 2015). However, current literature reviews show that for SPH turbulence, based on traditional turbulence models like RANS and LES, improvements made have not provided a comparable level of fidelity when compared to laminar SPH simulations.

4.3.2 Initial Simulation Data and Results

4.3.2.1 Evaluation of Velocity Results

4.3.2.1.1 Channel Flow

In this section, the flow pattern inside an infinitely long channel is investigated to test the capability of SPH in prediction of the velocity profile. In this study, a constant driven-body force acceleration is set to be $0.5m/s^2$, and the viscosity is modified, resulting in different Reynolds number. Periodic boundary is set, and the simulation is run for a sufficiently long time such that the flow will reach the fully developed region. Because the fluid particles in the layer are in contact with the surface of the boundary, the flow will gradually slow down and, finally, stop due to the non-slip condition. Due to the viscosity of the fluid, the layer in contact with the boundary will also slow down adjacent layers, thus gradually developing a velocity gradient across the cross-section of channel.

Low Reynolds Number (Re=25)

First of all, simulation with low Reynolds number is executed. In such cases, an analytical solution (Eq. 1) can be found for the velocity profile at steady-state conditions. NEUTRINO (NEUTRINO n.d.) and LAMMPS (LAMMPS-SPH n.d.) were chosen as the SPH simulation tools used in these studies, while STAR-CCM was selected as a cross-reference of mesh-based simulation methods. The comparison plot can be found in Figure 6.

$$u(y) = -\frac{1}{2v}\frac{dp}{dx}(a^2 - y^2)$$

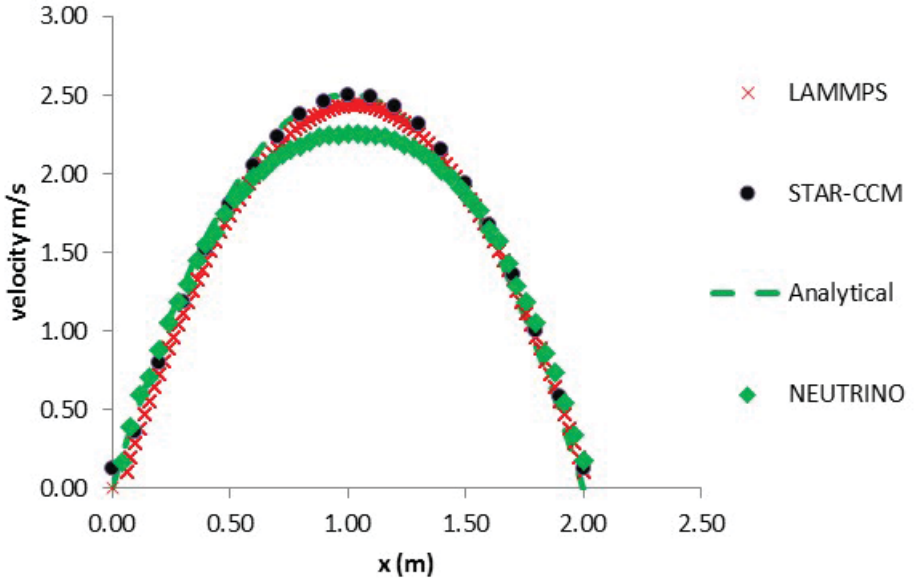

Figure 6. Comparison of low Re velocity profiles from different computational packages with the analytic solution.

A good agreement is found among the outputs. Other examples with low Reynolds number, including flow around a cylinder, Poiseuille flow, can be found in past work (Lin 2016). SPH is shown to be quite reliable for low-Reynolds cases.

4.3.2.2 Evaluation of Vortex

4.3.2.2.1 Lid-driven Flow

Lid-driven flow investigates the flow pattern within a closed square. The fluid is driven by moving the top side of the boundary at a constant velocity while keeping the other three walls stationary. Usually under these conditions, when the Reynolds number is high enough, a large vortex will form in the box with some small ones in corners. Because the pattern of the vortices is different for laminar and turbulent flow, and there are plenty of data available for validation (Ghia, Ghia and Shin 1982), lid-driven flow is simulated by SPH with low-to-high Reynolds number, and the performance is evaluated. In this study, a square box with $1m$ length and $1m/s$ driven velocity is set. The Reynolds number is modified by changing the viscosity value.

Low Reynolds Number (Re=1)

Simulations with low Reynolds number were performed. A good agreement is found between the SPH and mesh-based simulations as demonstrated in Figure 7.

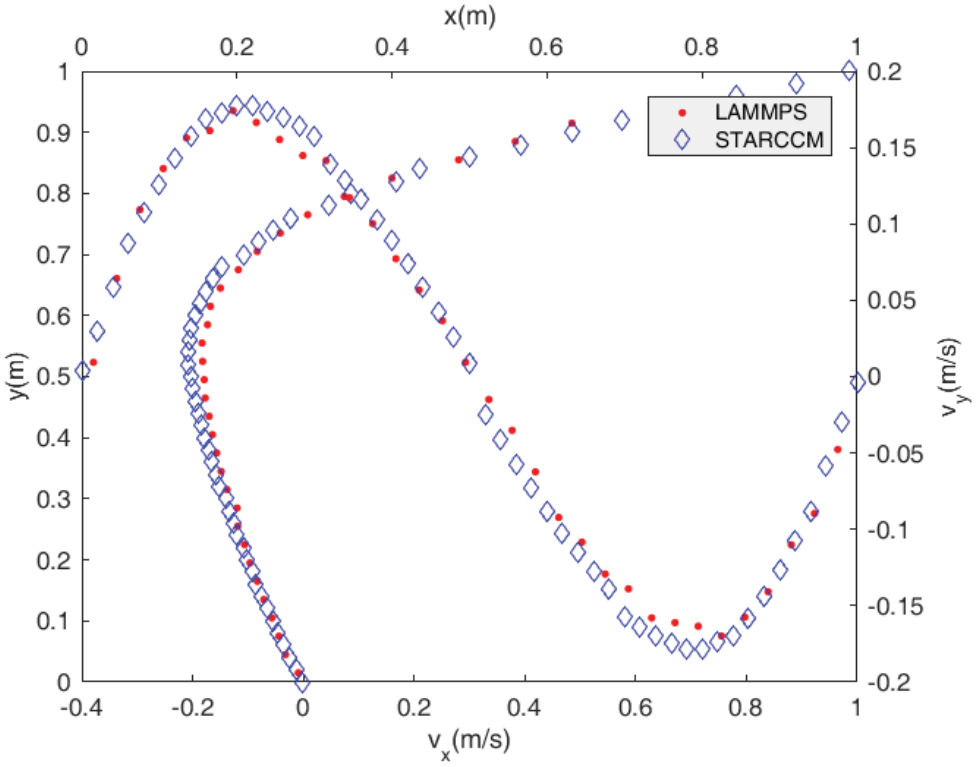

Figure 7. Velocity profile in horizontal and vertical centerline with Re = 1.

Medium (Re=100) and High (Re=1000) Reynolds Number

In this section, simulations with Reynolds number equal to 100 and 1000 are performed to demonstrate the capability of capturing vortex in high Reynolds cases. Comparisons are also made with different resolution to demonstrate the impact of particle sizes. Results are presented in Figures 8–11 below.

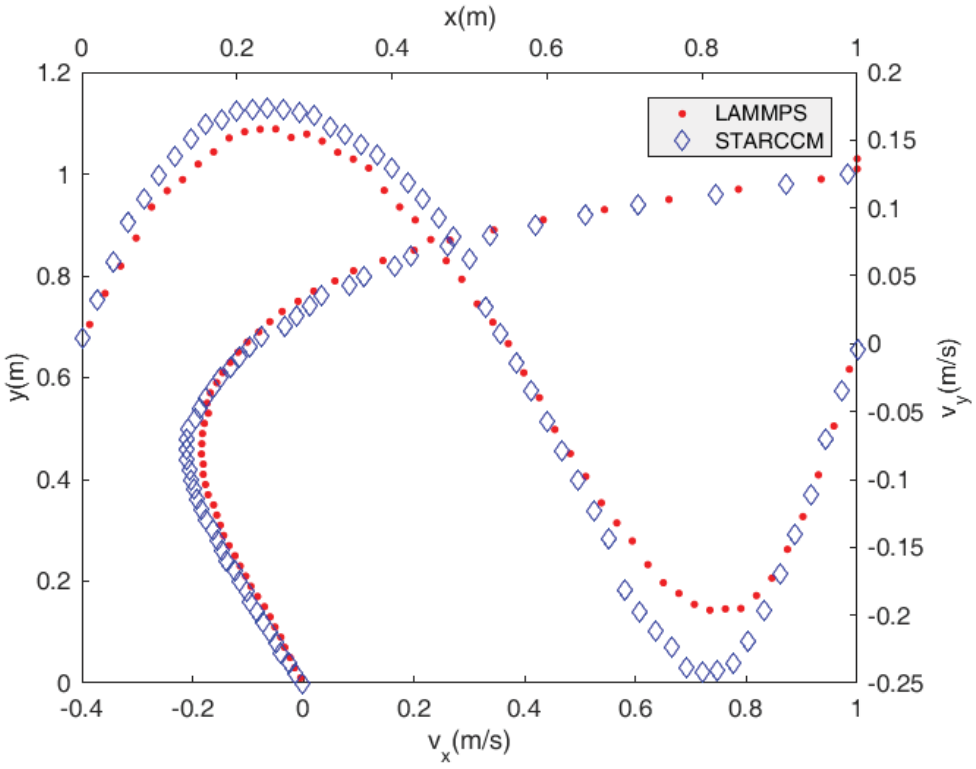

Figure 8. Velocity profile on the horizontal and vertical centerline with Re = 100,

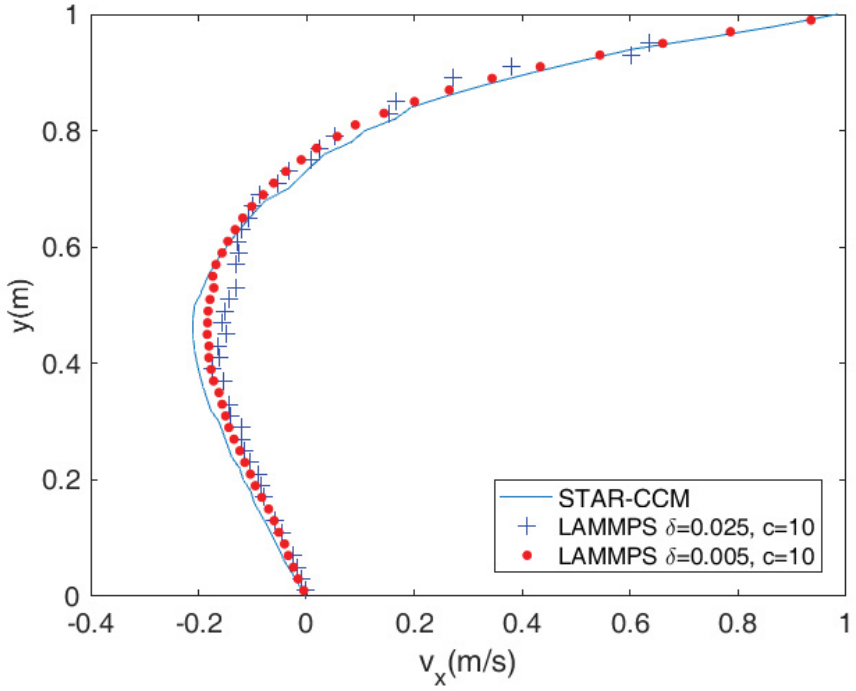

Figure 9. Velocity profile of different particle size on the vertical centerline with Re = 100.

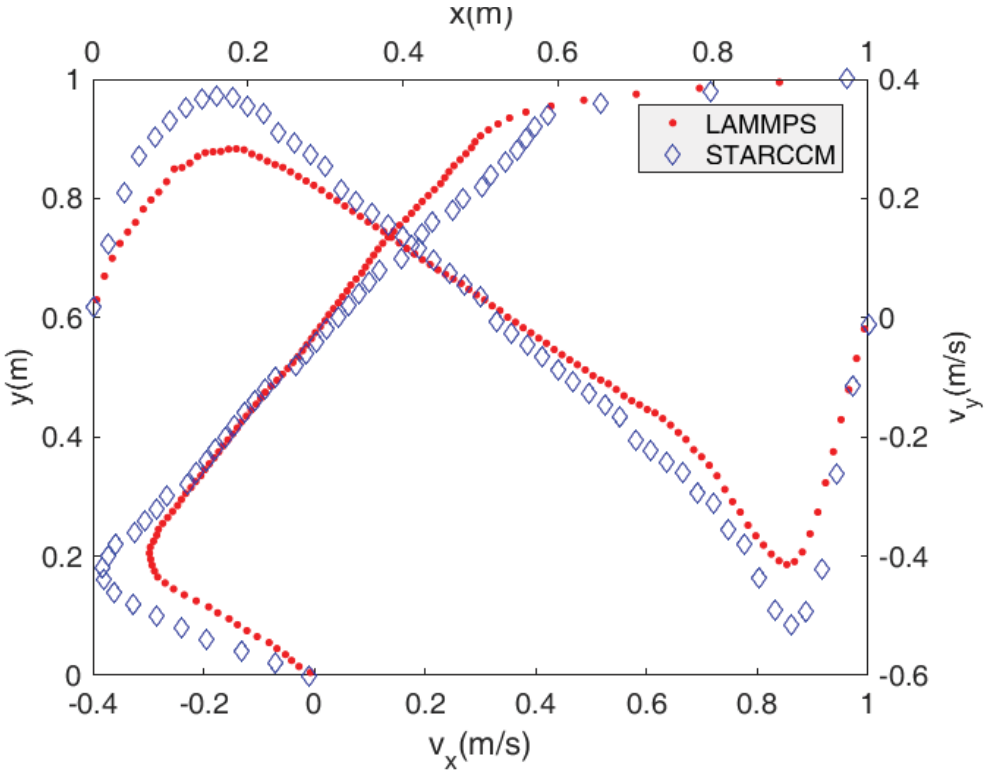

Figure 10. Velocity profile on the horizontal and vertical centerline with Re = 1000.

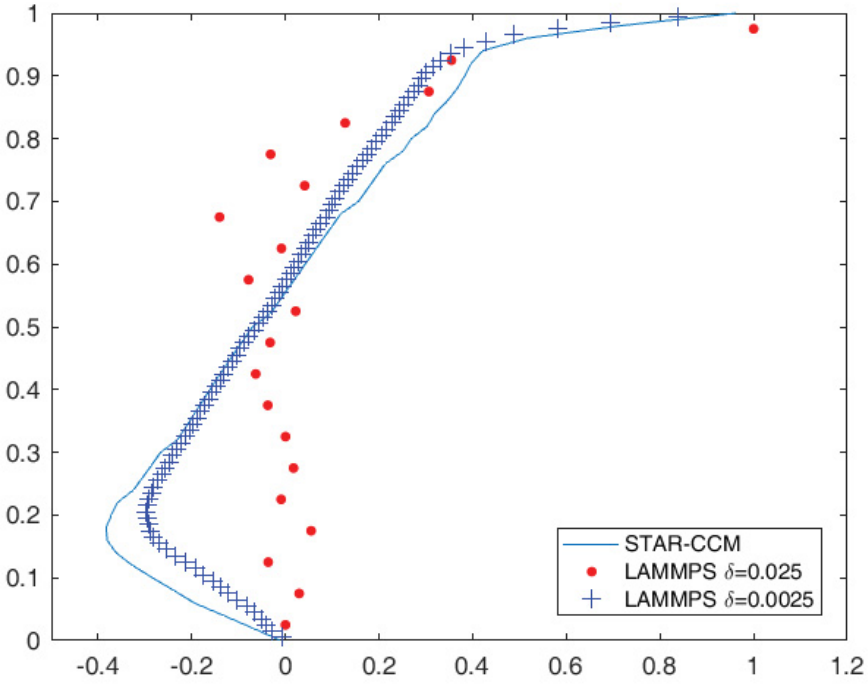

Figure 11. Velocity profile of different particle size on the vertical centerline with Re = 1000.

As indicated in Figure 8 (Re = 100) and Figure 10 (Re = 1000), with the same particle size as for the low-Reynolds case, the observed discrepancy grows with increasing Reynolds number. Also as shown in Figure 9 (Re = 100) and Figure 11 (Re = 1000), when particle size is refined and particle number increased, better results are obtained. This effect can be most clearly seen in Figure 11. Because SPH directly solves the Navier-Stokes equation, it can be treated as DNS when the particle size is small enough. However, the computational cost also grows with the refining of particle size and, because SPH doesn't have adaptive particle-size capability, it loses some of the advantage of SPH in computational speed when compared with use of mesh-based methods. A new way to improve SPH accuracy while maintaining low-cost computation is required. This could be achieved by building turbulence and more sophisticated boundary models.

As a result, SPH shows the capability of capturing vortices in fluid problems. However the accuracy degrades as the level of turbulence in the flow (as measured by the Reynolds number) increases. The particle size plays an important role in the results' accuracy because SPH becomes a type of DNS when the resolution is high enough. Since it's hard to achieve adaptive particle size in SPH, fluid models or closure laws may be needed to improve the accuracy while keeping the computational cost acceptably low.

4.3.2.3 Evaluation of Static Objects

4.3.2.3.1 Channel Flow with Block

In a high-wind simulation, flow over static obstacles is one of the important scenarios representing the wind traveling over and around buildings. A simple case, as shown in Figure 12, is built in both the NEUTRINO and STARCCM codes. In addition, a $k-\epsilon$ model is applied in STARCCM. Air properties are applied in each simulation with density $\rho = 1.225 kg/m^3$ and kinematic viscosity $\upsilon = 1.48 \times 10^{-5}\ m^2/s$. The velocity quiver plots from both programs are shown in Figure 13.

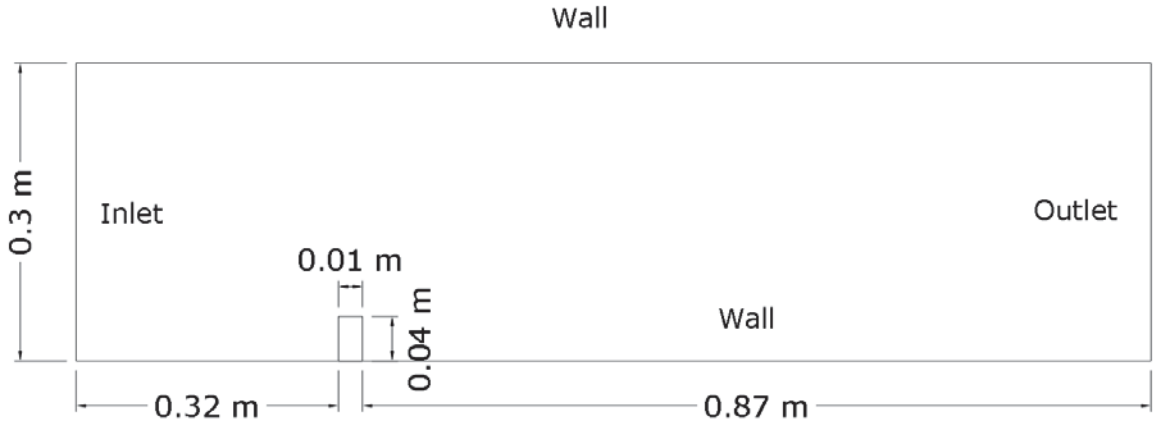

Figure 12. Setup and dimensions of channel flow with block.

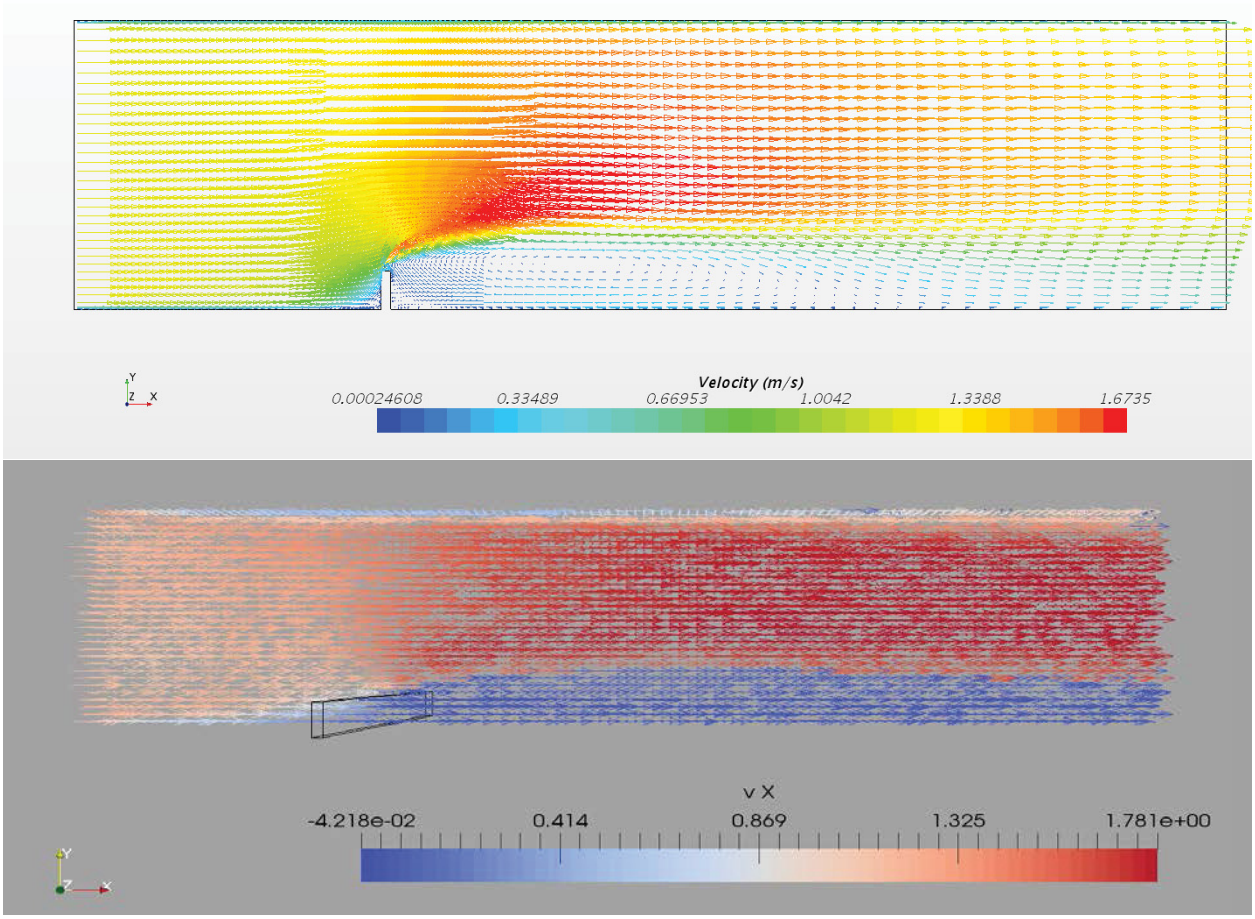

Figure 13. Velocity quiver plots from STARCCM with $\boldsymbol{k-\epsilon}$ model (upper) and NEUTRINO (lower).

The velocity profile along a vertical straight probe is extracted and plotted. Figure 14 and Figure 15 show the velocity plots before and behind the block, respectively. SPH accurately represents most of the velocity profile before and behind the obstacle, but details near the obstacle are missing (i.e., the regions inside the red box of Figure 14 and Figure 15).

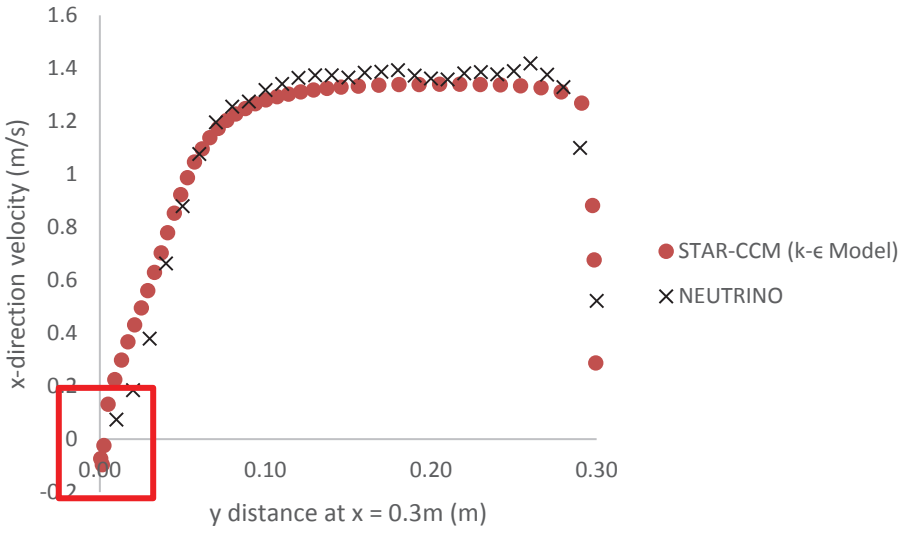

Figure 14. Velocity profile along vertical line in front of the block at x = 0.3 m.

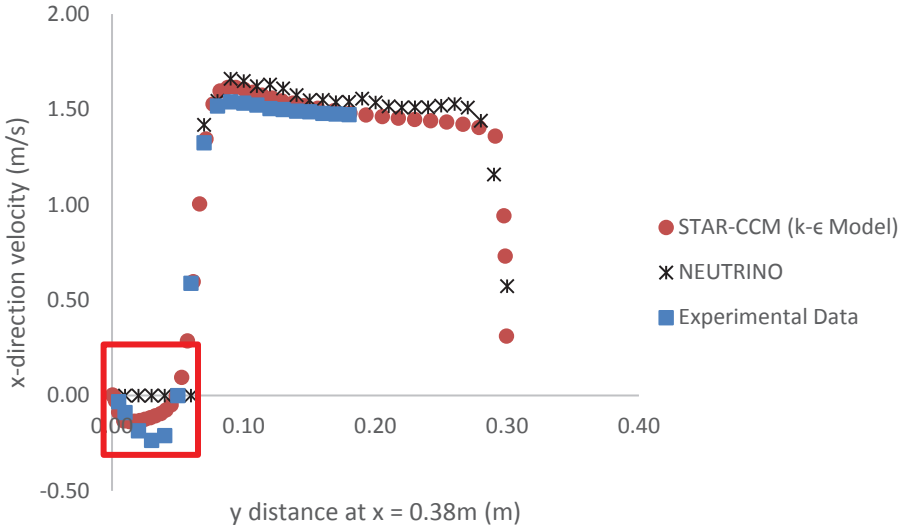

Figure 15. Velocity profile along vertical line behind the block at x = 0.38 m.

4.3.2.3.2 Evaluation of Moving Solids

One of the advantages of SPH over grid-based methods is its simple fluid-solid interaction. As stated earlier, debris in high-winds simulations are a concern for SSCs. The following sections demonstrate this capability; however, validation for wind-driven solids will need to be performed at a future point.

Moving Solids in Winds

In this simulation, a dynamic block with density $\rho = 10kg/m^3$ is introduced in the steady state of the former wind simulation. Then the block will move with the flow until it reaches the outlet. Figure 16 shows the plot at three time points.

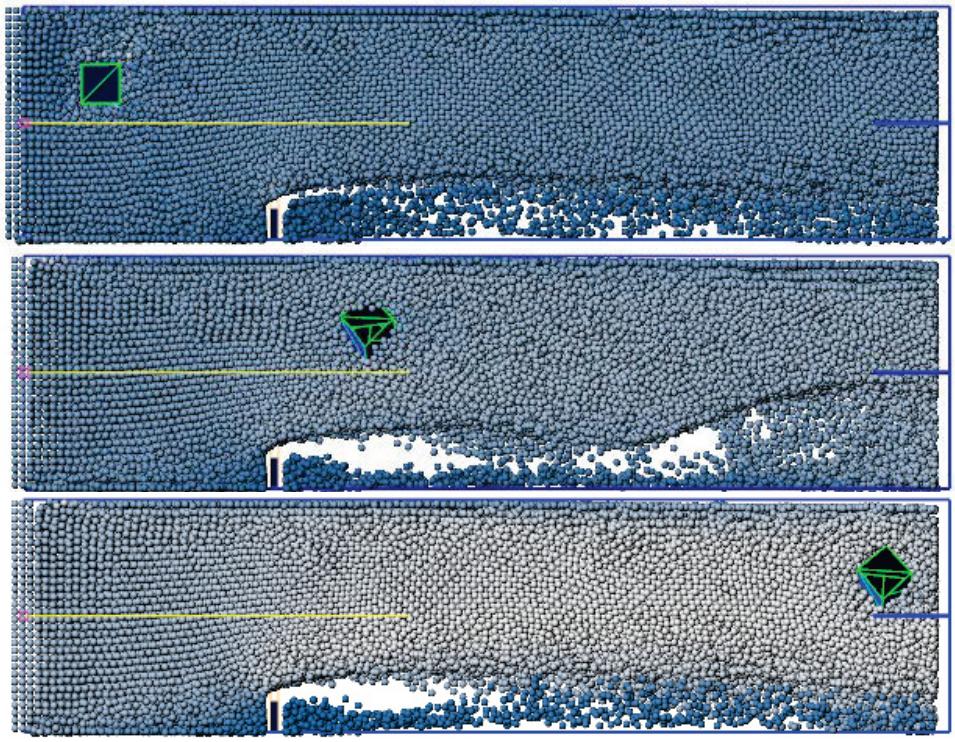

Figure 16. Demonstration of moving solids in wind.

Moving Solids in Fluid

In order to evaluate the accuracy of moving solids in a flow field, simulations with falling and floating blocks in a fluid are set and executed. Because of the existence of gravity, the block is initially held at the top of the tank until the fluid is stabilized under the effect of gravity. Figure 17 shows the transient plots of falling blocks from simulations conducted using the LAMMPS and NEUTRINO codes. Figure 18 shows the quiver plots from both packages at 2 seconds. Figure 19 shows the transient plot of the block's vertical displacements calculated using both computational packages. It turns out that although NEUTRINO's fluid simulation tends to be more viscous and stable than LAMMPS, there is still a nice agreement because gravity will dominate the process (when contrasted to the effects due to fluid viscosity).

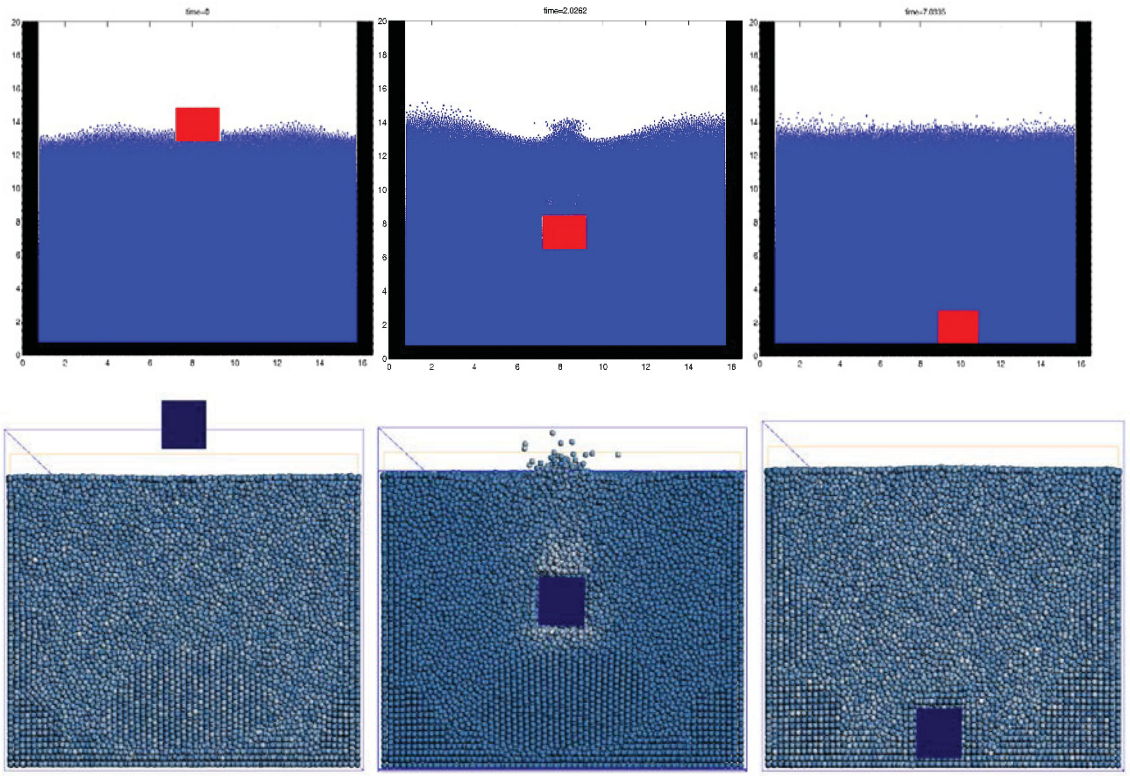

Figure 17. Transient plots of falling solids in fluid from LAMMPS (upper) and NEUTRINO (lower) at t = 0, 2, and 5 sec.

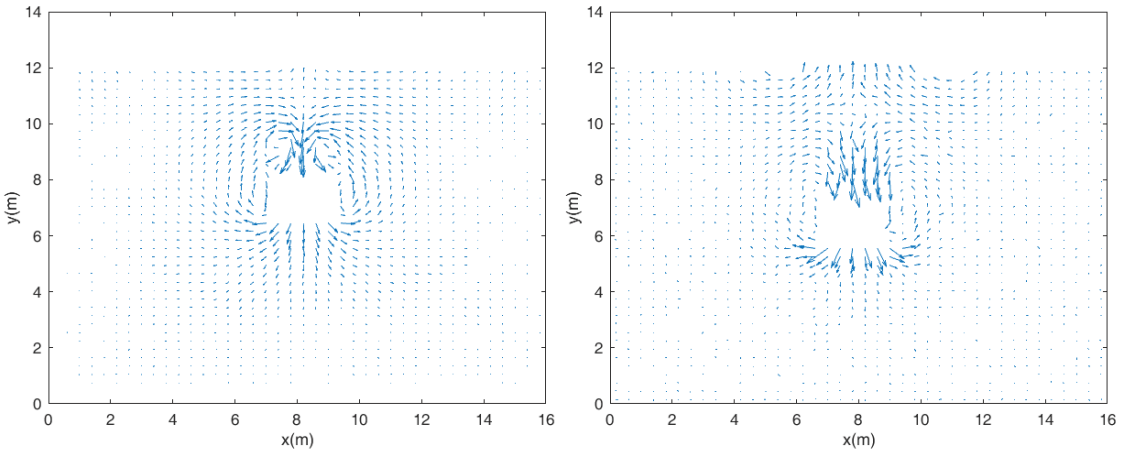

Figure 18. Quiver plot of falling solids in fluid from LAMMPS (left) and NEUTRINO (right) at t = 2 sec.

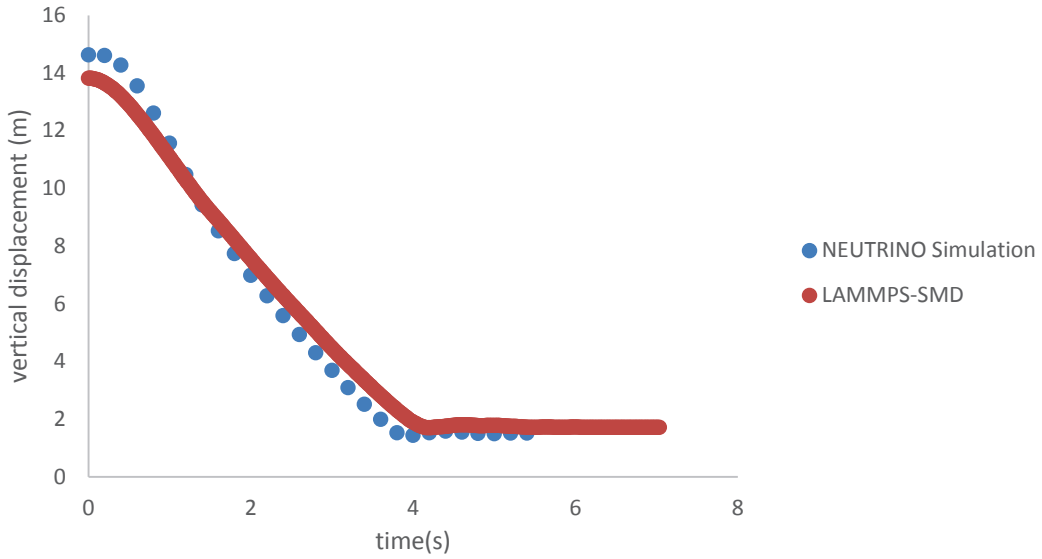

Figure 19. Comparison of vertical displacement of falling block simulated by LAMMPS and NEUTRINO.

Figure 20 shows the transient plots of floating blocks from LAMMPS and NEUTRINO. The block is initially held at the bottom of the tank and released after the fluid is stabilized. Figure 21 shows the quiver plots from both packages. Figure 22 shows the time transient of the block's vertical displacements from both packages. Although the qualitative behavior is similar between the simulations from the two packages, there are significant discrepancies between the quantitative results. In the NEUTRINO simulation, the box tends to float faster than in the LAMMPS simulation. It is believed that this behavior is caused by the different viscosity models between the two packages. More investigations are needed to obtain better clarification of the artificial terms in the SPH formula, including pressure, viscosity, surface tension, and so on.

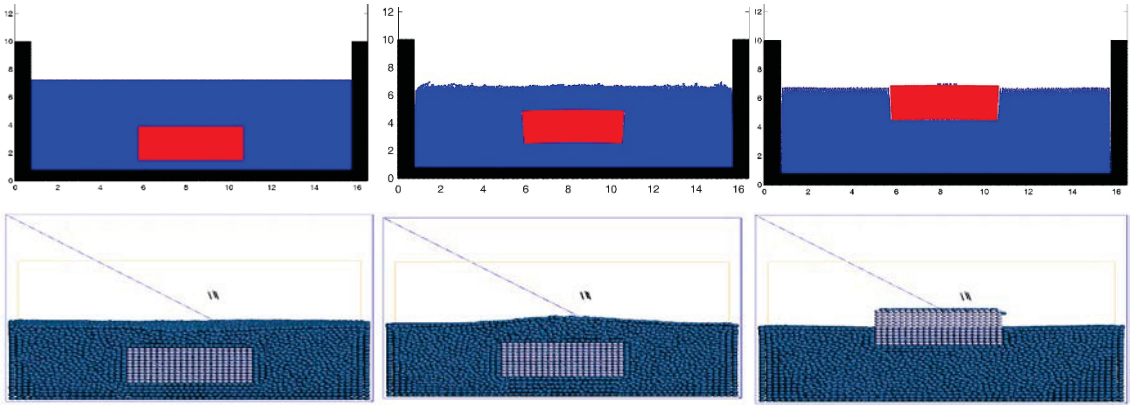

Figure 20. Transient plots of floating solids in fluid from LAMMPS (upper) at t = 0, 2, and 11 sec and NEUTRINO (lower) at t = 0, 0.46, and 11 sec.

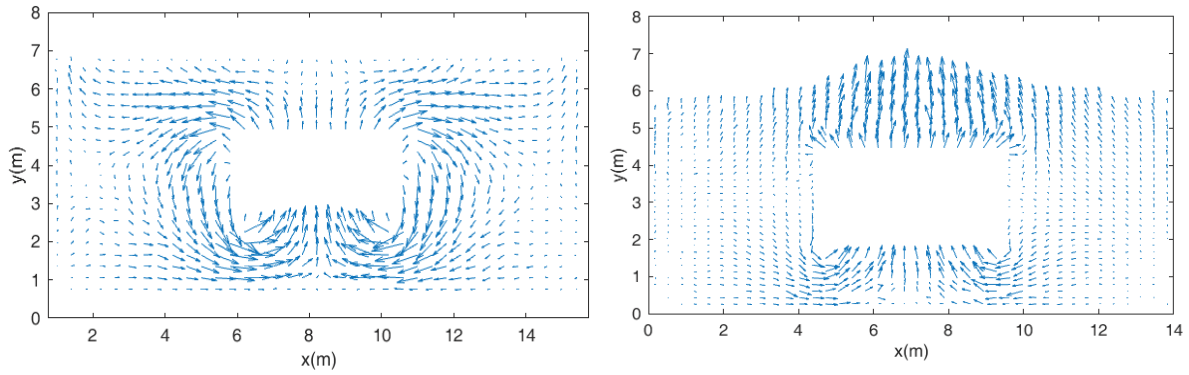

Figure 21. Quiver plot of falling solids in fluid from LAMMPS (left) at t = 2 ec and NEUTRINO (right) at t= 0.46 sec.

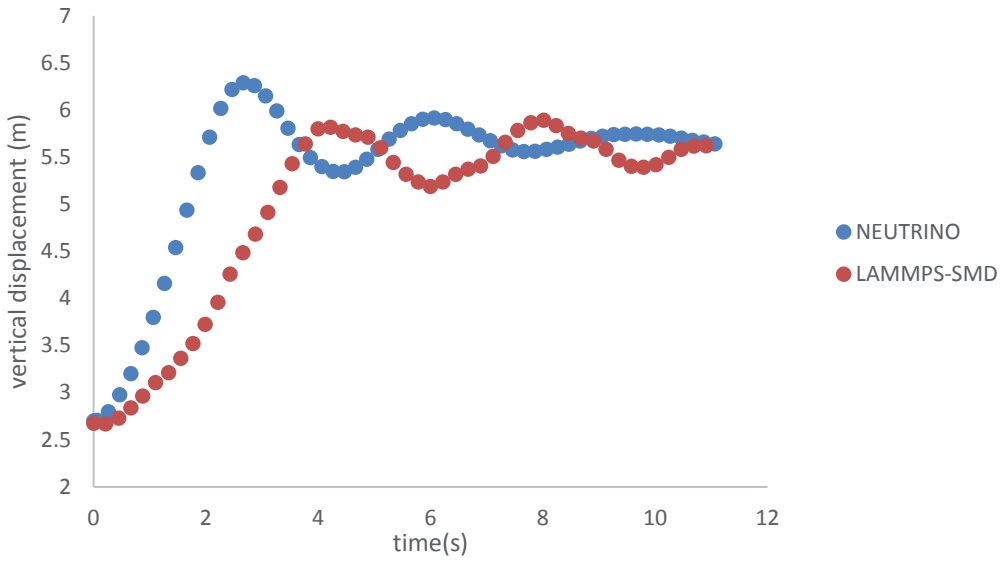

Figure 22. Comparison of vertical displacement of floating block simulated by LAMMPS and NEUTRINO.

In general, these SPH simulations demonstrate the capability of the approach to accurately simulate flow with both static and dynamic objects. Additionally, the moving trajectory of solids within a fluid can also be captured. From these initial simulations, it can be concluded that SPH has the capability of simulating floating objects suspended in a wind field; however, more verification and validation (V&V) activities are needed.

4.3.3 Initial SPH Challenges

4.3.3.1 Simulation Voids

As shown inside the box on Figure 14 and Figure 15, details near the solid objects embedded within the flow field are missing. Large particle vacancies, as shown in the red box in Figure 23, are found behind the obstacle embedded in the flow field. Because the particles are flowing along the streamline, they tend to "fly" away from the region that has small velocity or vortices. For the region behind the block, where the fluid velocity is usually slow and away from the main streamline, particles will not stay in the area, and this may cause large vacancies to occur during the simulation.

This is a known problem in SPH when there is no gravity in the model. Several methods such as particle shifting (see Section 4.4.1) or a turbulence model (see Section 4.4.2) may help solve this problem.

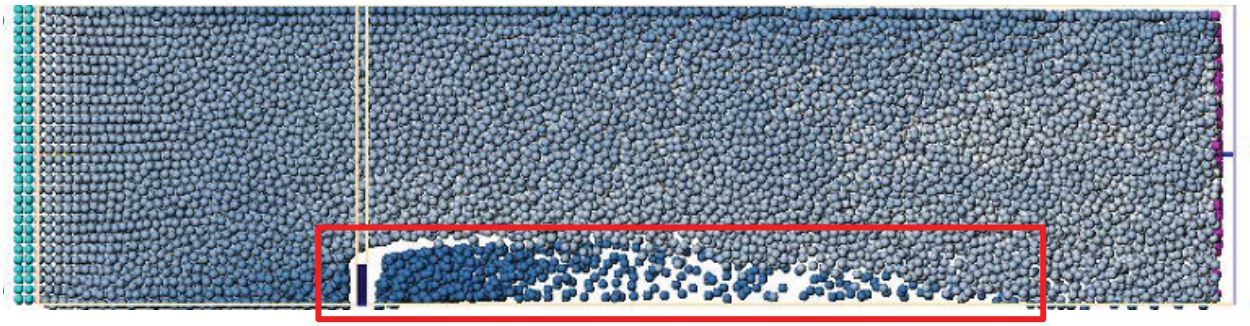

Figure 23. Particle distribution at 8 sec, particle vacancies, shown inside the red box, are found behind the block.

4.3.3.2 Domain and Particle Size

For application of SPH, the selection of particle size is critical in capturing all the phenomena of every scenario, and this becomes especially important in turbulent-flow regimes. Because the traditional SPH formulation directly solves the Navier-Stokes equation, it is treated as one of the DNS methods. Thus, the particle size needs to be smaller than the Kolmogorov-length scale (Prosperetti and Tryggvason 2007), which indicates the smallest eddy size in turbulent flow must be

$$\eta = \left(\frac{\nu^3}{\epsilon}\right)^{1/4}$$

where ν is the kinematic viscosity of the fluid, and ϵ is the average rate of dissipation of turbulence kinetic energy per unit mass. Usually, for atmospheric motion in which the large eddies have length scales on the order of kilometers, Kolmogorov length ranges from 0.1 to 10 millimeters (George 2011). However, simulation with such number of particles are extremely computationally expensive; thus closure laws are needed to model the effect of eddies, the sizes of which are smaller than the particle sizes, on the flow fields. Turbulence models like LES and RANS are closure models designed for single-phase high-Reynolds simulations.

4.4 SPH Path Forward

4.4.1 SPH Particle Shifting

SPH suffers from particle deficiencies in scenarios which would typically occur during wind driven flows, as indicated in Figure 23. This happens because particles in flow usually follow streamlines which result in particle vacancies behind obstacles in the flow path. Also, when the particle distribution becomes highly anisotropic, they tend become deficient in their neighborhood. To combat this problem, there are some schemes for enhancement of stability and accuracy of both explicit and semi-implicit particle methods, categorized as particle-regularization schemes. These schemes tend to regularize the anisotropic distributions of particles prone to be formed due to the Lagrangian characteristics of particle methods. A typical technique is the particle-shifting scheme of Xu et al. (R. S. Xu 2009), which slightly shifts the particles to prevent anisotropic particle structures. A more generic version of this scheme is proposed by Lind et al. (Lind 2012)(PSA). This method is based on Fick's diffusion law and relies on a Taylor expansion for evaluation of particle quantities in new positions.

In general, PSA consists of two steps. In the first step, the shifting vector δr_i of particle i can be obtained from the following equation

$$\boldsymbol{\delta r_i = C\zeta R_i}$$

where C is a constant in the range of 0.01–0.1, ζ and R_i are the shifting magnitude and direction of particle i, which can be calculated as

$$\zeta = V_{max}\Delta t$$

and

$$R_i = \sum_{j=1}^{N} \frac{\overline{r_{ij}^2}}{r_{ij}^2} n_{ij}$$

where V_{max} is the maximal particle velocity, Δt is the timestep and r_{ij} is the spacing between particle i and particle j , $n_{ij}$is the unit displacement vector, and $\overline{r_i}$ is the average particle spacing in the neighborhood of particle i ($\overline{r_i} = N^{-1}\sum_1^N r_{ij}$).

In the second step, after the particles are shifted according to the equation $\delta \mathrm{r_i} = \mathrm{C}\zeta \mathrm{R_i}(1)$, field variables must be adjusted accordingly as

$$\psi_{i'} = \psi_i + \delta r_i.(\boldsymbol{\nabla}\psi_i)$$

where ψ_i and $\psi_{i'}$ denote the field variables such as density, pressure, velocity, and position before and after shifting.

A modified version of the particle-shifting algorithm as suggested by Lind et al. (Lind 2012) is currently being implemented as part of Neutrino-SPH to deal with wind-driven flows.

If the model is run with the additions in Neutrino-SPH to accommodate particle shifting, a significant difference results between the flow profiles. The areas void of particles seem to be now filled. Because the technique of particle shifting affects mainly free surface particles, significant flow characteristics which occur in the interior areas of fluids don't seem to be affected. Figure 24 through Figure 27 illustrate the difference in flow with and without particle shifting implemented. In each of these figures the simulation is shown without particle shifting on the left and with particle shifting on the right.

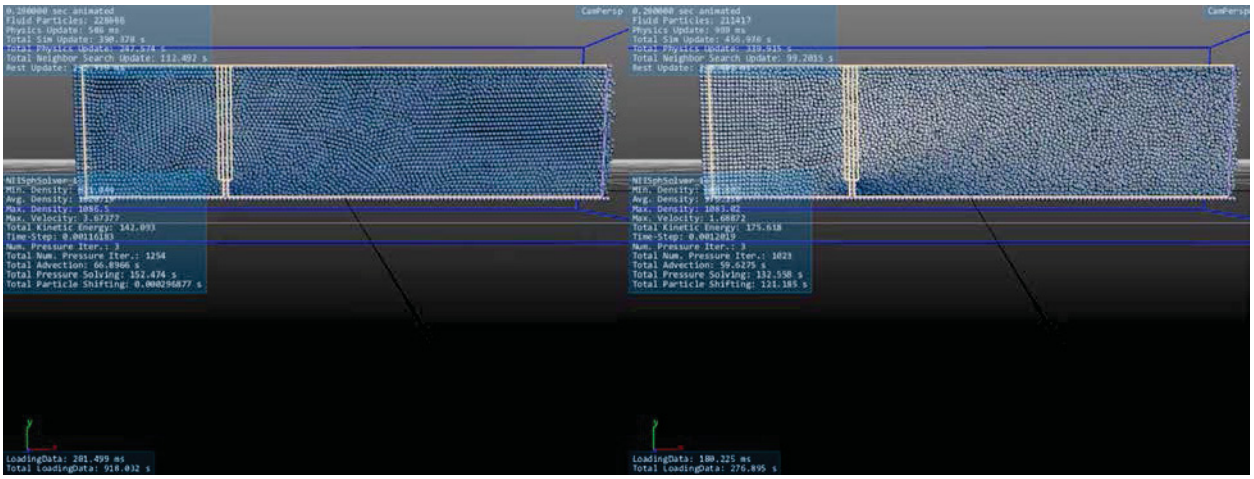

Figure 24. Beginning of simulation.

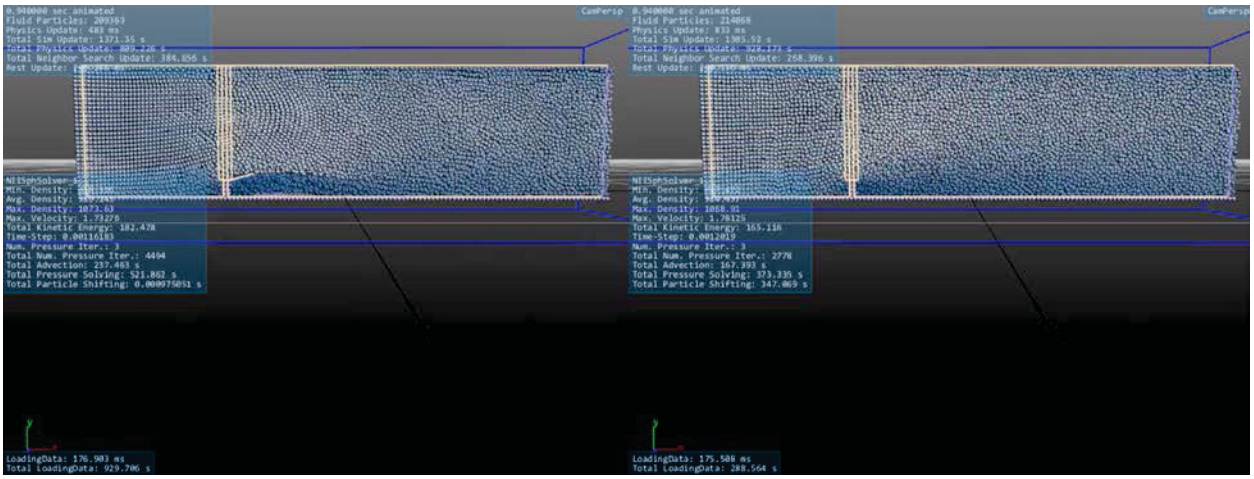

Figure 25. Simulation proceeds (particles accumulating along streamlines).

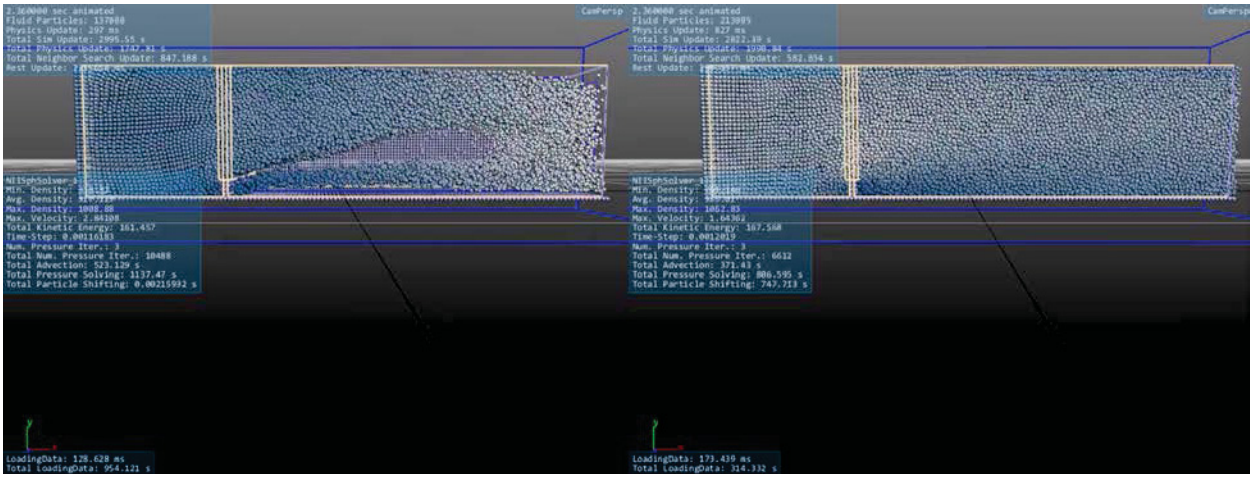

Figure 26. Progress of simulation (voids appearing).

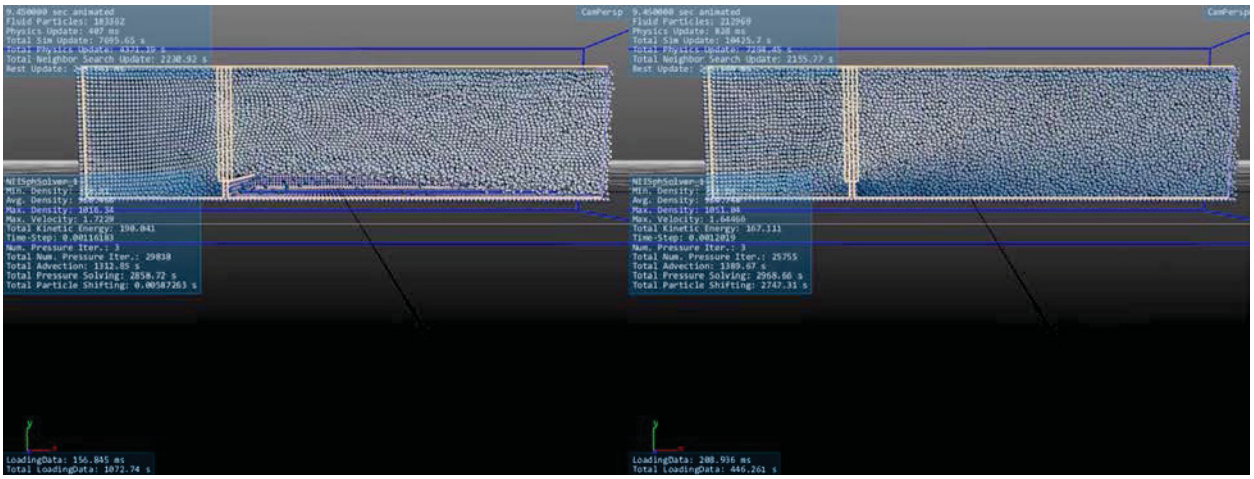

Figure 27: Steady flow (significant voids without particle shifting).

4.4.2 SPH Turbulence model

In early applications of SPH, 'violent' flows, with gravity and inertia dominating the simulations, were usually set. Traditionally, turbulence is not necessary for most SPH applications. However, for wind applications, the effects of gravity and inertia are relatively weak, and accurate predictions of velocity and force of the winds in the vicinity of buildings are needed. Thus, a turbulence model is needed for the capture of vortices and the boundary layer. Currently, there are two major types of turbulence models that can be used: large-eddy simulation (LES) and Reynolds-averaged Navier-Stokes (RANS). Because SPH interpolation is a kind of LES filter (Dalrymple and Rogers 2006), LES becomes a more relevant approach, and several successful simulations have been performed (Adami, Hu and Adams 2013). However, experience has indicated that it is difficult for SPH to deal with boundary layers using the LES approach, and the improvement observed has been limited (Mahmoudi, Zadeh and Ketabdari, A comparison between performaces of turbulence models on simulation of solitary wave breaking by WCSPH method 2014, Arai, Koshizuka and Murozono 2013).

On the other hand, RANS turbulence models have been widely applied in engineering applications with both linear and non-linear eddy viscosity models. In SPH, approaches with mixing length (Violeau, Piccon and Chabard 2002), k-ε model (Shao 2006) or explicit algebraic Reynolds stress models (Wallin and Johansson 2000) have been built and tested. It turns out that SPH turbulence with RANS generally provides better results and, considering the calculational expense, RANS models require coarser particle size and less computer power than LES. However, due to the introduction of closure models in RANS, initial and boundary conditions can greatly affect the solutions. For specific scenarios of application, the selection of different models also can impact the results because every turbulence model has its own assumptions, and high uncertainty will be introduced in the breakdown of specific model assumptions. For example, many RANS models are based on Boussinesq hypothesis:

$$\overline{u_i' u_j'} = \frac{2}{3} k \delta_{ij} - 2\nu_t S_{ij}$$

where u_i' is the ith component of the velocity-field fluctuations, k is the turbulent kinetic energy, ν_t is the eddy viscosity and S_{ij} is the mean strain-rate tensor. However, the Boussinesq hypothesis is only strictly correct in flows where the turbulent time scale is much smaller than the mean-shear-time scale; otherwise, the Reynolds stresses will be subject to non-local effects. Thus, in many engineering applications, some assumptions may be violated in various regions of the flow. Though there are some alternative closures that can avoid the deficiencies of the Boussinesq hypothesis, like Reynolds stress-transport models and LES, they are too computationally expensive to be smoothly used in engineering applications.

4.4.3 Data-driven model

In order to accurately predict flows without increasing computational expense, a data-driven turbulence model is proposed. Recently, some work has been done to improve the prediction of the Reynold stress term in standard RANS model (Ling and Templeton 2015, Wang, Wu and Xiao 2016). Researchers have investigated the use of offline data (existing benchmark data for flows different from that to be predicted (Dow and Wang 2011)), online data (streamed monitoring data from the flow to be predicted (Iungo, et al. 2015)), or a combination of both in a data-driven approach. In this study, SPH will become the targeting model and will be calibrated by high-fidelity models from mesh-based simulations.

A brief scheme of the model can be found in Figure 24. In this process q(x) represents spatial features, and the discrepancies in the vector field between SPH and the high-fidelity data Δ(x) is calculated. Then a regression function to relate q(x) and Δ(x) is built using standard regression techniques, which can be either deterministic (linear regression) or random (Gaussian process). In this work, random Forests regression is proposed because the mapping may not have an explicit form and is determined based on a number of decision trees. It is worth notice that the choice of flow features can greatly affect the final results and, due to the natural difference between particle-based and mesh-based

simulation, the quantities must be carefully selected. Ling (Ling and Templeton 2015) has recommended some possible non-dimensional inputs for turbulence modeling.

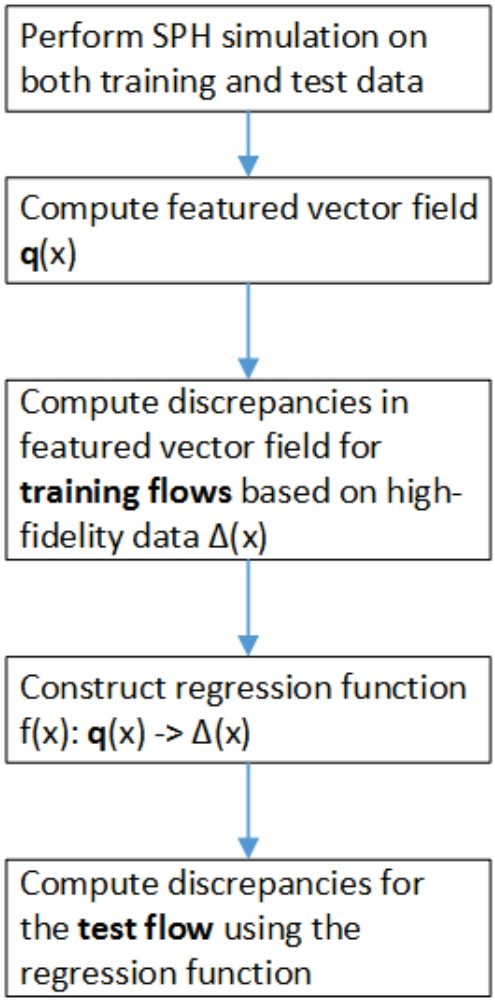

Figure 28. Scheme of data-driven turbulence model in SPH.

With the application of a data-driven turbulence model, the epistemic uncertainties from the empirical parameters in traditional turbulence models can be avoided. Because a sophisticated data-driven model is trained by high-fidelity results across a range of flow conditions, it avoids the breakdown of assumptions. Compared to a purely statistical regression model, a physics-based data-driven approach will be able to predict fluid flow while introducing less stochastic uncertainty. Also, because a data-driven model is trying to fix the region of SPH with low fidelity or performance, it saves more computing power than use of DNS or LES.

4.5 Conclusion

As a result of the 2011 accident at the Fukushima Dai-ichi NPP and other operational NPP experience, there is an identified need to better characterize and evaluate the potential impacts of externally generated hazards on NPP safety. Due to the ubiquitous occurrence of high winds around the world and the possible extreme magnitude of the hazard that has been observed, the assessment of the impact of the high-winds hazard has been identified as an important activity by both NPP owner-operators and regulatory authorities. However, recent experience obtained from the conduct of high-winds risk assessments indicates that such activities have been both labor-intensive and expensive to perform.

Additionally, the existing suite of methods and tools to conduct such assessments (which were developed decades ago) do not make use of modern computational architectures (e.g., parallel processing, object-oriented programming techniques, or simple user interfaces) or methods (e.g., efficient and robust numerical-solution schemes). As a result, the current suite of methods and tools will rapidly become obsolete.

Physics-based 3D simulation methods can provide information to assist in the RISMC PRA methodology. This research is intended to determine what benefits SPH methods could bring to high-winds simulations for the purposes of assessing their potential impact on NPP safety. The initial investigation has determined that SPH can simulate key areas of high-wind events with reasonable accuracy, compared to other methods. Some problems, such as simulation voids, need to be addressed, but possible solutions have been identified and will be tested with continued work. This work also demonstrated that SPH simulations can provide a means for simulating debris movement; however, further investigations into the capability to determine the impact of high winds and the impacts of wind-driven debris that lead to SSC failures need to be done.

SPH simulations alone would be limited in size and computation time. An advanced method of combing results from grid-based methods with SPH through a data-driven model is proposed. This method could allow for more accurate simulation of particle movement near rigid bodies even with larger SPH particle sizes. If successful, the data-driven model would eliminate the need for a SPH turbulence model and increase the simulation domain size. Continued research beyond the scope of this project will be needed in order to determine the viability of a data-driven model.

4.6 BIBLIOGRAPHY

Adami, S., X. Y. Hu, and N. A. Adams. 2013. "Simulating three-dimensional turbulence with SPH." *Proceedings of the Summer Program 2012* . Trondheim. 377-382.

ANS. 2012. *Fukushima Daiichi: ANS Committee Report.* Lagrange Park, IL: American Nuclear Society.

Arai, J., S. Koshizuka, and K. Murozono. 2013. "Large eddy simulation and a simple wall model for turbulent flow calculation by a particle method." *Internal Journal For Numerical Methods in Fluids* 772-787.

ASME. 2012. *Forging a New Nuclear Safety Construct – The ASME Presidential Task Force on Response to Japan Nuclear Power Plant Events.* New York: American Society of Mechanical Engineers.

ASME/ANS. 2013. *RA-Sb Standard for Level 1/Large Early Release Frequency PRA for NPP Applications.* American Society of Mechanical Engineers / American Nuclear Society.

C. Miller, A. Cubbage, D. Dorman, J. Grobe, G. Holahan, and N. Sanfilippo. 2011. *Recommendations for Enhancing Reactor Safety in the 21st Century – The Near-Term Task Force Review of Insights from the Fukushima Dai-ichi Accident.* SECY 11-0093, Washington: United States Nuclear Regulatory Commission.

C.L. Smith, S. Prescott, J. Coleman, E. Ryan, B. Bhandari, D. Sludern, C. Pope, and R. Sampath. 2015. *Progress on the Industry Application External Hazard Analyses Early Demonstration.* INL/EXT-15-36749, Idaho Falls: Idaho National Laboratory.

Dalrymple, R. A., and B. D. Rogers. 2006. "Numerical modeling of water waves with the SPH method." *Coastal Engineering* 141-147.

Dow, E., and Q. Wang. 2011. "Quantification of structural uncertainties in the k{! turbulence model." *52nd AIAA/ASME/ASCE/AHS/ASC Structures, Structural Dynamics and Materials Conference.* Denver: AIAA.

EPRI. 2015. *Identification of External Hazards for Analysis in Probabilistic Risk Assessment – Update of Report 1022997.* Report 3002005287, Palo Alto: Electric Power Research Institute.

EPRI. 1978. *Tornado Missile Risk Analysis.* EPRI NP-768, Palo Alto: Electric Power Research Institute.

Ferrand, M. 2011. "Unified semi-analytical wall boundary conditions for inviscid, laminar and turbulent slightly compressible flows in SPARTACUS-2D combined with an improved time integration scheme on the continuity equation." Manchester.

George, W. K. 2011. "Lectures in Turbulence for the 21st Century." *Turbulence Research Lab.* March 23. Accessed November 16, 2016. http://www.turbulence-online.com/Publications/Lecture_Notes/Turbulence_Lille/TB_16January2013.pdf.

Ghia, U., K. N. Ghia, and C. T. Shin. 1982. "High-Re solutions for incompressible flow using the Navier-Stokes equations and a multigrid method ." *Journal of Computational Physics* 387-411.

Hayes, John. 2011. *"The Historic Tornadoes of April 2011".* Silver Spring: U.S. National Oceanic and Atmospheric Administration.

Hebdon, F.J. 1993. *Effect of Hurricane Andrew on the Turkey Point Nuclear Generating Station from August 20-30, 1992.* NUREG--1474, Washington: United States Nuclear Regulatory Commission.

Huffman, K. 2011. *EPRI Fukushima Daini Independent Review and Walkdown.* Report 1023422, Palo Alto: Electric Power Research Institute.

IAEA. 2015. *The Fukushima Daiichi Accident – Report by the Inspector General.* Vienna: International Atomic Energy Agency.

Institute of Nuclear Power Operations. 2011. "Special Report on the Nuclear Accident at the Fukushima Daiichi Nuclear Power Station." INPO 11-005, Atlanta.

Iungo, G., F. Viola, U. Ciri, M. Rotea, and S. Leonardi. 2015. "Data-driven RANS for simulations of large wind farms." *Journal of Physics* 012025.

J. P. Gaertner, K. Canavan, and D. True. 2008. *Safety and Operational Benefits of Risk-Informed Initiatives.* Report 1016308, Palo Alto: Electric Power Research Institute.

J.C. Sciaudone, L.A. Twisdale, S.S. Banik, and D.R. Mizzen. 2015. "High Wind Plant PRA Walkdown Insights and Recommendations." *Proceedings of PSA2015.* Lagrange Park: American Nuclear Society.

Justin Coleman, Chandu Bolisetti, Swetha Veeraraghavan, Carlo Parisi, Steven Prescott, Abhinav Bupta, Annie Kammerer. 2016. *Multi-Hazard Advanced Seismic Probabilistic Risk Assessment Tools and Applications.* INL/EXT-16-40055, Idaho Falls: Idaho National Lab.

K. Hope, N. Povroznyk, and R. Schneider. 2015. "Tornado Missile Strike Calculator." *PSA2015.* Lagrange Park: American Nuclear Society.

K. Huffman, P. Bruck, T. Esselman, and P. Streeter. 2012. *Fukushima Daiichi Accident – Technical Causal Factor Analysis.* Report 1024946, Palo Alto: Electric Power Research Institute.

L. A. Twisdale, W. L. Dunn. 1983. *Probabilistic Analysis of Tornado Wind Risks.* J. Struct. Eng (1983) 109 pp. 468-488, Raleigh: American Society of Civil Engineers.

L. Shanley, D. Miller. 2011. *Identification of External Hazards for Analysis in Probabilistic Risk Assessment.* EPRI Report 1022997, Palo Alto: Electric Power Research Institute.

L.A. Twisdale, N. Lovelace, and C. Slep. 2015. "High Wind PRA Failure Calculations, Error Estimates and Use of CAFTA." *PSA2015.* Lagrane Park: American Nuclear Society.

L.A. Twisdale, P.J. Vickery, J.C. Sciaudone, S.S. Banik, and D.R. Mizzen. 2015. "Advances in Wind Hazard and Fragility Methodologies for HW PRAs." *PSA2015.* Lagrange Park: Smerican Nuclear Society.

Laboratories, Sandia National. n.d. "How to PIRT." Albuquerque.

n.d. *LAMMPS-SPH.* http://lammps.sandia.gov.

Leroy, A. 2015. *A new incompressible SPH model : towards industrial applications.* Paris: University Paris-Est.

Lin, L. 2016. *Assessment of the smoothed particle hydrodynamics method for nuclear thermal-hydraulic applications.* Raleigh: North Carolina State Uninversity.

Lind, S., Xu, R., and Stansby P. 2012. "Incompressible smoothed particle hydrodynamics for free-surface flows: A generalised diffusion-based algorithm for stability and validations for impulsive flows and propagating waves[J]." *Journal of Computational Physics* 1499-1523.

Ling, J., and J. Templeton. 2015. "Evaluation of machine learning algorithms for prediction of regions of high Reynolds averaged Navier Stokes uncertainty." *Physics of Fluids.*
Lovelace, A. Mironenko and N. 2015. "High Wind PRA Development and Lessons Learned from Implementation." *PSA2015.* Lagrange Park: American Nuclear Society.
Lucy, Leon B. 1977. "A Numerical Approach to Testing the Fission Hypothesis." *The Astronomical Journal* 82(12):1013-1924.
Mahmoudi, A., H. H. Zadeh, and M. J. Ketabdari. 2014. "A comparison between performaces of turbulence models on simulation of solitary wave breaking by WCSPH method." *Journal of Civil Engineering and Urbanism.*
Mahmoudi, A., H. H. Zadeh, and M. J. Ketabdari. 2014. "A Comparison between Performances of Turbulence Models on Simulation of Solitary Wave Breaking by WCSPH Method." *Journal of Civil Engineering and Urbanism* 4 (1): 1-7.
Monaghan, J.J. 2005. "Smoothed particle hydrodynamics." *Reports on Progress In Physics* (Institute of Physics Publishing) 1703-1759.
Monaghan, R.A. Gingold and J.J. 1977. "Smothed particle hydrodynamics: theory and application to non-spherical stars." *Monthly notices of the Royal Astronomical Society* 181:375-398.
n.d. *NEUTRINO.* http://www.neutrinodynamics.com.
NRC. 2014. *Bounding Generic Risk Assessment for Selected Plant Systems Portions of Which are not Protected from Tornado-Generated Missiles.* Washington: United States Nuclear Regulatory Commission.
NRC. 2014. *Bounding Generic Risk Assessment for Selected Plant Systems Portions of Which are not Protected from Tornado-Generated Missiles.* Washington: United States Nuclear Regulatory Commission.
NRC. 2016. *Browns Ferry Nuclear Power Plant Licensee Event Report to U.S. NRC 50-259/2011-002-00.* Washington: United States Nuclear Regulatory Commission ADAMS.
NRC. 2011. *Design Basis Hurricane and Hurricane Missiles for Nuclear Power Plants.* Regulatory Guide 1.221, Washington: United States Nuclear Regulatory Commission.
NRC. 2001. *Design Basis Tornado and Tornado Missiles for Nuclear Power Plants.* Regulatory Guide 1.76, Washington: United States Nuclear Regulatory Commission.
NRC. 1994. *Effect of Hurricane Andrew on Turkey Point Nuclear Generating Station and Lessons Learne.* Information Notice 93-53 Supplement 1, Washington: United States Nuclear Regulatory Commission.
NRC. 1993. *Effect of Hurricane Andrew on Turkey Point Nuclear Generating Station and Lessons Learned.* Information Notice 93-53, Washington: United States Nuclear Regulatory Commission.
NRC. 2015. *Enforcement Discretion for Tornado-Generated Missile Protection Noncompliance.* NRC Enforcement Guidance Memorandum (EGM) 15-002, Washington: United States Nuclear Regulatory Commission.
NRC. 1991. *Individual Plant Examination of External Events (IPEEE) for Severe Accident Vulnerabilities.* 10CFR 50.54(f) (Generic Letter No. 88-20, Supplement 4), Washington: United States Nuclear Regulatory Commission.
NRC. 2002. *Perspectives Gained from the Individual Plant Examination of External Events (IPEEE) Program.* NUREG 1742, Washington: United States Nuclear Regulatory Commission.
NRC. 1983. *PRA Procedures Guide – A Guide to the Performance of Probabilistic Risk Assessments for Nuclear Power Plants.* NUREG/CR-2300, Washington: United States Nuclear Regulatory Commission.
NRC. n.d. *Prioritization of Recommended Actions to be Taken in Response to Fukushima Lessons Learned.* SECY 11-0137, Washington: United States Nuclear Regulatory Commission.
NRC. 1975. *Reactor Safety Study – An Assessment of Accident Risks in U.S. Commercial Nuclear Power Plants.* WASH-1400 (NUREG 75/014), Washington, DC: United States Nuclear Regulatory Commission.

NRC. 2007. *Tornado Climatology of the Contiguous United States.* NUREG/CR-4461 Revision 2, Washington: United States Nuclear Regulatory Commission.
NRC. 2015. *Tornado Missile Protection.* NRC Regulatory Issue Summary (RIS) 2015-06, Washington: United States Nuclear Regulatory Commission.
NRC. 2005. *Transient and Accident Analysis Methods.* Regulatory Guide 1.203, Washington: U.S. Nuclear Regulatory Commission.
NRC. 2008. *Use of TORMIS Computer Code for Assessment of Tornado Missile Protection.* NRC Regulatory Issue Summary (RIS) 2008-14, Washington: United States Nuclear Regulatory Commission.
Prosperetti, A., and G. Tryggvason. 2007. *Computational methods for multiphase flow.* New York: Cambridge Press.
Ramprasad Sampath, Niels Montanari, Nadir Akinci, Steven Prescott, Curtis Smith. 2016. "Large-Scale Solitary Wave Simulation with Implicit Incompressible SPH." *Journal of Ocean Engineering and Marine Energy* (Journal of Ocean Engineering and Marine Energy) 313-329.
Shao, S. 2006. "Incompressible SPH simulation of wave breaking and overtopping with turbulence modeling." *International Journal for Numerical Methods in Fluids* 597-621.
U.S. National Oceanic and Atmospheric Administration. 2011. *The Historic Tornadoes of April 2011.* Silver Spring, MD: U.S. National Oceanic and Atmospheric Administration.
Union of Concerned Scientists. 2011. "Hurricane Andrew vs. Turkey Point." *allthingsnuclear.* July 12. Accessed Oct 25, 2016. http://allthingsnuclear.org/dlochbaum/fission-stories-48-hurricane-andrew-vs-turkey-point.
Violeau, D., S. Piccon, and J. P. Chabard. 2002. "Two attempts of turbulence modelling in smoothed particle hydrodynamics." *Advances in Fluid Modelling and Turbulence Measurements.* World Scientific. 339-346.
Wallin, N., and A. V. Johansson. 2000. "An explicit algebraic Reynolds stress model for incompressible and compressible turbulent flows." *Journal of Fluid Mechanics* 89-132.
Wang, J. X., J. L. Wu, and H. Xiao. 2016. "Physics-Informed machine learning for predictive turbulence modeling: using data to improve RANS modeled Reynolds Stresses." *Physical Review of Fluids.*
Wierman, T. E. 2013. *Analysis of Loss-of-Offsite-Power Events 1998–2012.* INL/EXT-14-31133, Idaho Falls: Idaho National Labratory.
Xu. n.d.
Xu, R., Stansby, P., & Laurence, D. 2009. "Accuracy and stability in incompressible SPH (ISPH) based on the projection method and a new approach." *h. Journal of Computational Physics, 228(18)* 6703–6725.